ABSTRACT

QUAN, LAN TU. Electrochemistry of Cytochrome *c* on Self-Assembled Phosphonic Acid Terminated Alkanethiols on Gold. (Advised by Professor Edmond F. Bowden)

The synthesis of 10-mercaptodecanylphosphonic acid (C_{10}PA) and self-assembly of C_{10}PA on gold electrodes are reported. The electrochemical characterization of cytochrome *c* (cyt *c*) adsorption on the C_{10}PA self-assembled monolayer (SAM) and on mixed hydroxyl(OH)/phosphonic acid (PA) terminated SAMs is also described, and a comparison is made to the pure carboxylic acid (COOH) SAM. On the pure C_{10}PA SAM, no electroactivity for adsorbed cyt *c* was obtained. This lack of electroactivity could be due to a lack of adsorption resulting from hydrogen binding among the diprotic phosphonic acid groups, which could act to limit ionization needed for electrostatic cyt *c* binding at the interface. Alternatively, it could be that cyt *c* does bind strongly to this SAM, but becomes denatured or oriented in an unfavorable position for electron transfer to take place. On the other hand, cyt *c* electroactivity was obtained on the mixed OH/PA SAMs. In the mixed SAM, the OH terminated alkanethiol serves as a hydrophilic diluent, spacing out the phosphonic acid groups and thus limiting their ability to engage in mutual hydrogen bonding. Studies undertaken to examine the effects of OH alkanethiol chain length, the mole ratio of OH/PA, and self-assembly time yielded an optimal set of conditions for cyt *c* electroactivity, namely a 10:1 ratio C_{11}OH/C_{10}PA mixed SAM prepared with a 2 hour assembly time. Under those conditions, the redox properties of adsorbed cyt *c* were determined and compared with results for the widely studied COOH SAM. The formal potentials obtained for horse cyt *c* for both the C_{11}OH/C_{10}PA mixed SAM and the C_{10}COOH pure SAM were approximately 230 mV vs

NHE. The surface coverage for both types of monolayer were ~ 10 pmol/cm^2. The electron transfer rate constants obtained were 17.7 s^{-1} and 12.7 s^{-1} for $C_{11}OH/C_{10}PA$ mixed SAM and $C_{10}COOH$ pure SAM, respectively. Overall, the redox properties of cyt *c* on $C_{11}OH/C_{10}PA$ mixed SAM were found to be similar to those obtained for a pure $C_{10}COOH$ SAM of comparable thickness.

Electrochemistry of Cytochrome *c* on Self-Assembled Phosphonic Acid Terminated Alkanethiols on Gold

By

Lan Tu Quan

A thesis submitted to the Graduate Faculty of
North **C**arolina **S**tate **U**niversity
in Partial fulfillment of the
requirements for the Degree of
Master of Science

Department of Chemistry
Analytical Division

Raleigh, North Carolina

2004

Approved by:

_____	_____
Morteza G. Khaledi	Tatyana I. Smirnova

_____
Edmond F. Bowden
Chair of Advisory Committee

This work is dedicate to loving family

Dad, Mom, Nam, Phuong, and Kevin

Thank you for your abundant love and encouragement. I love you all!

BIOGRAPHY

Lan Tu Quan was born in Rach Gia, Viet Nam on May 2, 1977 to Chau and Hue Quan. Her family moved to the United States in hoping to provide a better education and better life for her and her siblings. She has one sister (Phuong) and two brothers (Nam & Kevin). Lan attended Matthews Elementary in Greenwood, SC, where she first learned English and made her first contact with Americans. Lan adapted to the American lifestyle and environment very quickly and made lots of friends. Her English speaking skills progressed very fast and so has her southern accent. Shortly, after graduated from Emerald High, she attended the University of South Carolina, where she first became interest in chemistry. In spring 2001, she graduated with a Bachelor of Science degree in Chemistry and a minor in Biology. The following fall of 2001 she started her journey in graduate school at the North Carolina State University.

ACKNOWLEDGEMENTS

I would like to thank my parents for always being there encouraging and supporting everything I do. Thanks for always believing in me. I also like to thank my brothers and sister for always being there for me when I needed them. I am so proud to be a part of this family. Your unconditional love had giving me so much strength, courage, and joy. Thank you!

Tremendous thanks are given to my advisor Dr. Ed Bowden who has guided and developed me and taught me to think like a scientist. I have learned so much from you and am looking forward to learn more. Thank you!

Much gratitude is extended to Justin Youngblood for helping me to learn the techniques of organic synthesis and making organic chemistry as easy as cooking a meal. Treating this as cooking had successfully leaded me to synthesize the molecule that I needed for my research. Thank you!

Much appreciation is extended to Christopher Njue for giving me good advice and engaging in useful discussions on my research. Thank you!

For all of my friends, thank you for your friendships. You had made my life more meaningful. Especially Yuee Feng, you are truly a rare friend. Thank you for the amazing time here. I will always cherish those happy memories. Also I would like to acknowledge Luat Vu for his help with drawing some of the most wonderful figures in this thesis and thank you for motivated me when I feel like giving up. That means a lot to me. Thank you!

TABLE OF CONTENTS

LIST OF FIGURES

Chapter 1

Chapter 3

Chapter 4

LIST OF SCHEMES

Chapter 2

LIST OF REACTIONS

Chapter 1

Chapter 2

LIST OF EQUATIONS

Chapter 3

Chapter 4

LIST OF TABLES

Chapter 4

CHAPTER 1

Introduction and Background

1.1. INTRODUCTION AND BACKGROUND

Self-assembled monolayers (SAMs) are stable single molecule layers of reasonably well-defined chemical composition formed on solid or liquid substrates by self-assembly methods. Since Nuzzo and Allara[1] reported that organosulfur molecules such as octadecanethiol, $HS(CH_2)_{17}CH_3$, and other alkane thiols can spontaneously assemble into stable and highly organized molecular layers on gold surfaces in 1983, the study of SAMs has expanded tremendously. Organosulfur molecules, usually thiols or disulfides, bond to gold surfaces through the sulfur atom resulting in an organic surface defined by the terminal group. This monolayer system is widely studied because it is relatively simple, highly stable, and easy to prepare. A simple model of a SAM is depicted in Figure 1.1.

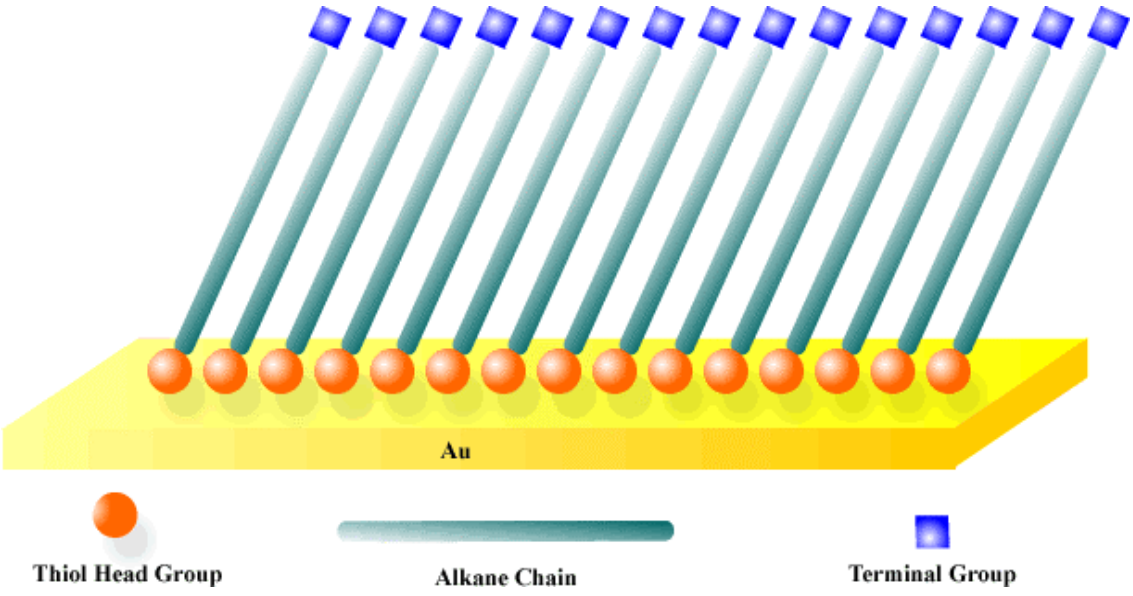

Figure 1.1. Model of self-assembled monolayer on gold electrode.

The ability to tailor both the chain length and the terminal functionality of the constituent molecules makes the SAM an excellent candidate for modeling natural processes such as transmembrane electron transfer, cellular recognition, and immunological protection[2], and also in areas such as wetting[3,4] , lubrication[5], adhesion[6] , corrosion[7,8] , and chemical sensing[9]. Changing the functional group at the terminal end of the thiol alters the chemical as well as physical characteristics of SAM surfaces. Such functional group control allows the composition of SAM surfaces to be tailored for specific applications.

There have been many studies conducted using SAMs as biological surface mimics to investigate the electron transfer reactions of redox proteins. Proteins adsorbed directly on metal electrodes are typically not stable and tend to undergo irreversible denaturation[10,11]. To eliminate surface-induced denaturation, SAMs have been used to impart surface chemistry compatible with stable protein adsorption[12]. The most extensively studied protein/SAM combination has been cytochrome *c* (cyt *c*) on carboxylic acid (COOH) terminated SAMs[13-15]. The first report on the direct electron transfer between cytochrome *c* and any type of modified gold electrode was by Eddowes and Hill[16] in 1977. Also at the same time, Yeh and Kuwana's[17] work on cyt *c* at tin-doped indium oxide electrodes was reported. Both groups obtained quasi-reversible diffusional cyclic voltammetry for solution-resident cyt *c*. Since then cyt *c* has been the most popular choice for studying redox proteins on SAMs. Cytochrome *c* is a well-characterized electron transfer (ET) protein with a notably asymmetric distribution of surface charge. A number of positively charged lysine amino acid residues reside near the exposed heme edge, which is the binding site for negatively charged protein partners.

The positively charged lysine patch of cyt *c* interacts electrostatically with negatively charged SAMs[12], thus providing a model electrochemical system for studying fundamental properties of biological electron transfer processes.

A particularly important molecular group in biology is the phosphate group. Phosphates serve essential roles in membrane structure, cellular signal transduction, energy metabolism, genetic information storage, and bone structure[18]. It is a key building block for many essential intracellular compounds such as nucleic acids, phospholipids, and enzymes. Oxyphosphorus based compounds have been examined by different method for the different use and fundamental knowledge. Most oxyphosphorus compounds (phosphates and phosphonates) studies are related to biological systems due to that phosphorus present in the biological macromolecules such as DNA, RNA, and ribozymes[19].

To date, most studies of redox proteins adsorbed on SAMs that are terminated with carboxylic acid or other functional groups have been carried out[20], but none on organophosphate or phosphonate terminated SAMs. There exists one study in which phosphonic acid alkanethiol SAMs were used for investigating blood compatibility[2]. However, there are no reports of successful redox protein electrochemistry using organophosphate or phosphonate terminated surfaces.

In this thesis, phosphonate compounds served as a starting point. Phosphonates and organophosphates are structurally similar. An organophosphate has 4 oxygens with an alkyl group connected via a phosphoester bond. Phosphonates have 3 oxygens with a carbon attached directly to phosphorus (Figure 1.2). The lack of a hydrolyzable P-O-C

linkage makes phosphonate compounds more stable in aqueous solution and easier to make than organophosphate compounds.

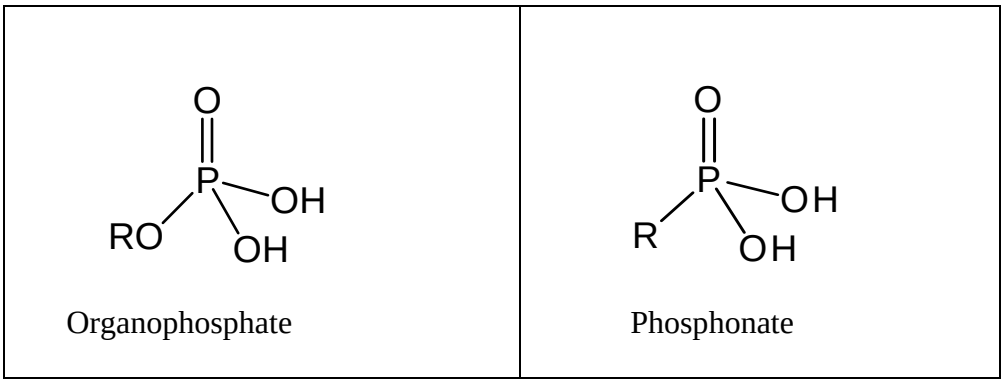

Figure 1.2. Structure of organophosphate and phosphonate compounds.

The main focus of this research is to gain a deeper understanding of interfacial interactions and charge transfer between proteins and phosphate modified SAM surfaces. It is proposed that surface with phosphorus containing groups such as phosphate or phosphonate can give some insight as to the role of phosphorus based groups on interfacial biological processes with cyclic voltammetry technique.

The specific tasks comprising this research are as follows: (1) synthesis and self-assembly of phosphonate terminated thiols on gold electrodes; (2) electrochemistry of adsorbed cyt *c* on phosphonate terminated SAMs on gold electrode; (3) electrochemistry of adsorbed cyt *c* on mixed SAMs of phosphonate and hydroxyl terminated thiols.

1.2. SELF-ASSEMBLED MONOLAYERS

The self-assembled monolayer (SAM) has become a widely studied model system for investigating electron transfer between surfaces and redox molecules. SAMs were not given much attention until the 1980s. In the self-assembly method, alkanethiols, $HS(CH_2)_nX$, usually in the form of thiols, disulfides, or sulfides are spontaneously assembled onto gold or other metals upon exposure of the metal surface. SAMs can be prepared that are highly stable, densely packed and ordered. The SAM-metal electrode system shown in Figure 1.1 shows that attachment occurs through the sulfur atom. The sulfur is strongly bonded to the working metal electrode surface. The binding energy of sulfur to gold is approximately 160 kJ/mol[21]. Thiolate SAMs have been formed on electrodes such as gold[14], silver[13], copper[22], platinum[23], tin oxide[24], and mercury[25]. Gold is the most popular choice of substrate since SAMs formed on platinum are less stable and both silver and copper are air sensitive. Silver and copper tend to form an oxide layer when exposed to air.

Upon exposure to an alkanethiol containing solution, molecules rapidly attach to the metal substrate through the sulfur end. In a polar solvent, the alkane chains become attract to each other due to dispersion forces and solubility differences. Then, over a longer time frame, the alkane chains can undergo rearrangement and become aligned in a roughly parallel and upright orientation on the electrode surface to maximize the dispersion interactions[26]. The chain tilt angle depends on the terminal group and the substrate that is used[20]. An angle of approximately 30^o has been reported for unsubstituted alkanethiols self-assembled on Au(111)[20]. One advantage of using SAMs

is that the alkane chain length can also be easily modified, thus creating films of variable thickness. Longer alkane chains will have greater dispersion interactions than shorter chains, thus leading to a lower free energy and a more ordered monolayer[20]. Another advantage of SAMs is that the terminal group can be modified to realize specific binding of target redox molecules. Some examples of terminal groups reported in the literature include carboxylic acid, alcohol, ester, amide, amine, and nitrile.

1.3. CYTOCHROME *c*

Mitochondrial cytochrome *c* (cyt *c*) is the most studied electron transfer protein and it has been extensively characterized[12, 15]. The cytochrome *c* from horse is composed of 104 amino acids[27,] , is water soluble and weighs approximately 12,500 Daltons. Its shape is roughly ellipsoidal with dimensions of 30 Å x 34 Å x 30 Å. Cyt *c* plays an important role as an electron carrier in the mitochondrial intermembrane space between two membrane bound protein complexes, cyt *c* reductase and cyt *c* oxidase[12]. Its redox center is a heme group positioned off-center with one edge partially exposed to solution. The heme iron is complexed with four nitrogen atoms of the porphyrin ring while two amino acids, histidine-18 and methionine-80, serve as axial ligands (Figure 1.3).

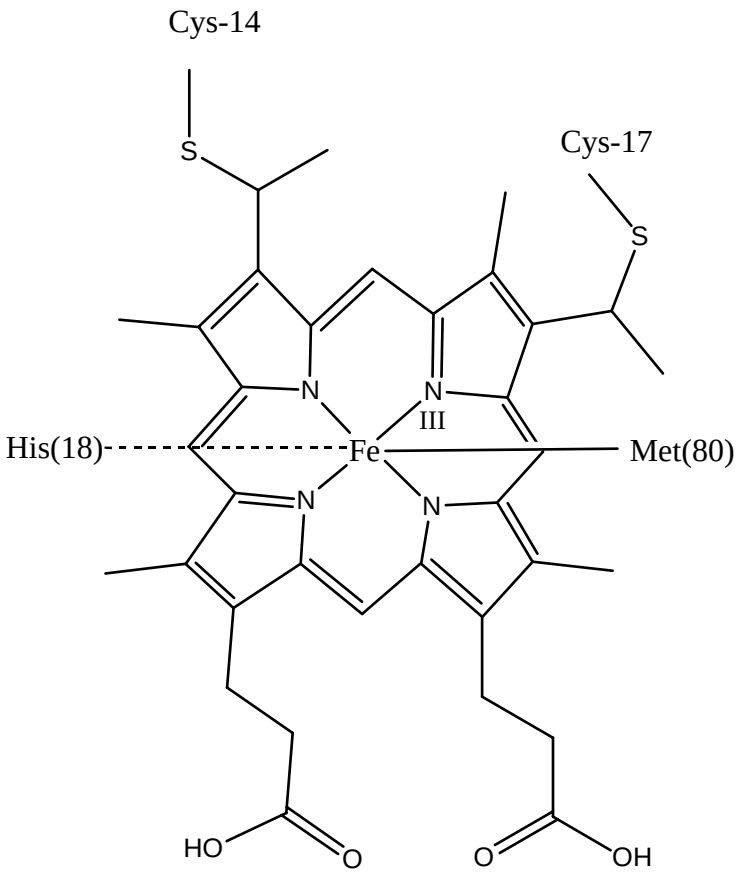

Figure 1.3. Structure of cytochrome *c* heme with two axial ligands, histidine-18 and methionine-80.

The heme iron of cyt *c* is normally in a low spin six-coordinate state and cycles between the ferrous (Fe^{2+}) and ferric (Fe^{3+})[12] oxidation states (Reaction 1.1).

$$Fe^{3+} + e^{-} \rightleftharpoons Fe^{2+}$$

(**Reaction 1.1**)

As mentioned earlier, the cyt *c* surface charge distribution is asymmetric (Figure 1.4). Cyt *c* has 21 positively charged residues (19 lysines and 2 arginines) distributed over most of the protein surface including the heme edge region. The backside of cyt *c*, opposite the heme edge, however, serves as the primary location of the12 glutamate and aspartate residues, which act to neutralize the backside cation charges. This give rise to an exposed heme edge region with an excess positive charge[12].

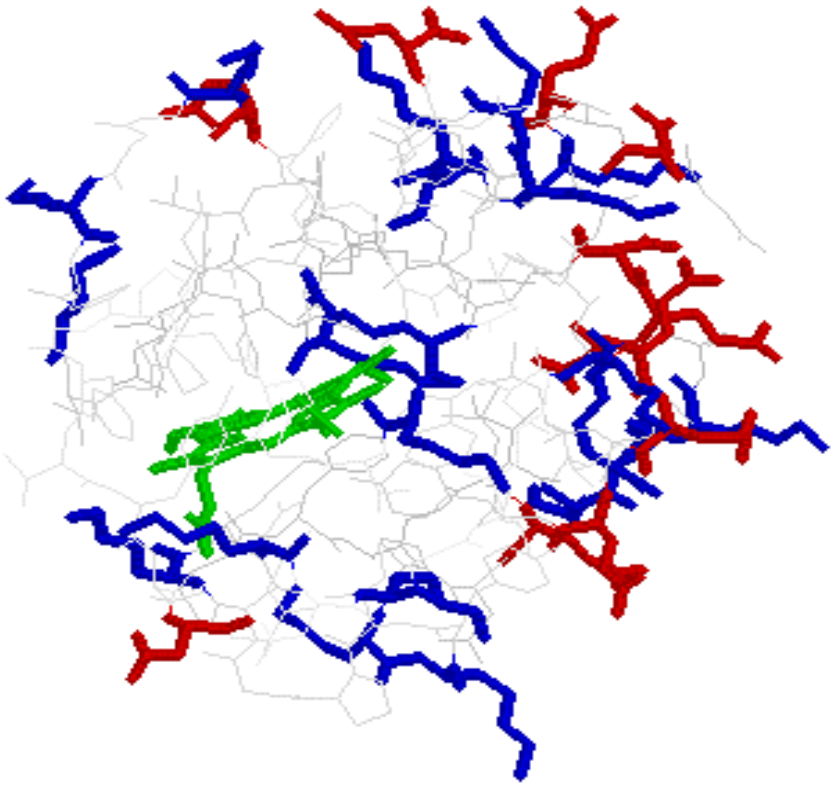

Figure 1.4. Crystal structure of cytochrome *c* depicting the excess positive charged on the heme side of the molecule. Positively charged lysine and arginine amino acids (blue) and negatively charged glutamate and aspartate amino acids (red) are depicted. The heme is noted in green. The structure was obtained from the Protein Data Bank under the protein code 1HRC[28].

Because of this charge distribution, negatively charged functionalities on an electrode surface can have strong electrostatic interactions with the positively charged heme edge side of cyt *c*[14, 29, 30]. This makes cyt *c* an excellent choice to study protein electron transfer on negatively charged electrode surfaces that feature carboxylate groups. Surface distribution of charges is depicted in Figure 1.5.

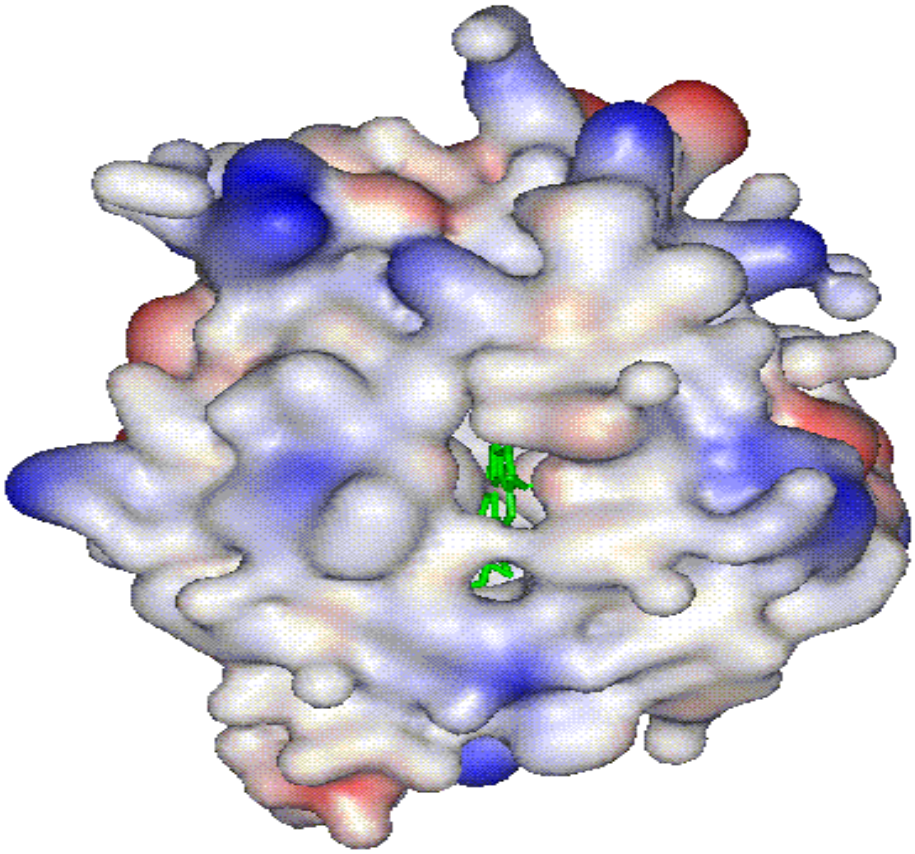

Figure 1.5. Structure of cyt *c* illustrating the surface charge distribution. Blue represents positively charged lysine and arginine. Red represents the negatively charged glutamate and aspartate. The heme is represented in green. The structure was obtained from the Protein Data Bank under the protein code 1HRC[28]

Niki and coworkers proposed that lysine-13 specifically controls the interfacial electron transfer kinetics of horse cyt *c*[31]. They found that the interfacial electron transfer rate was 5 orders of magnitude lower when lysine-13 was replaced with alanine. Figure 1.6 shows the location of lysine-13 relative to the heme group.

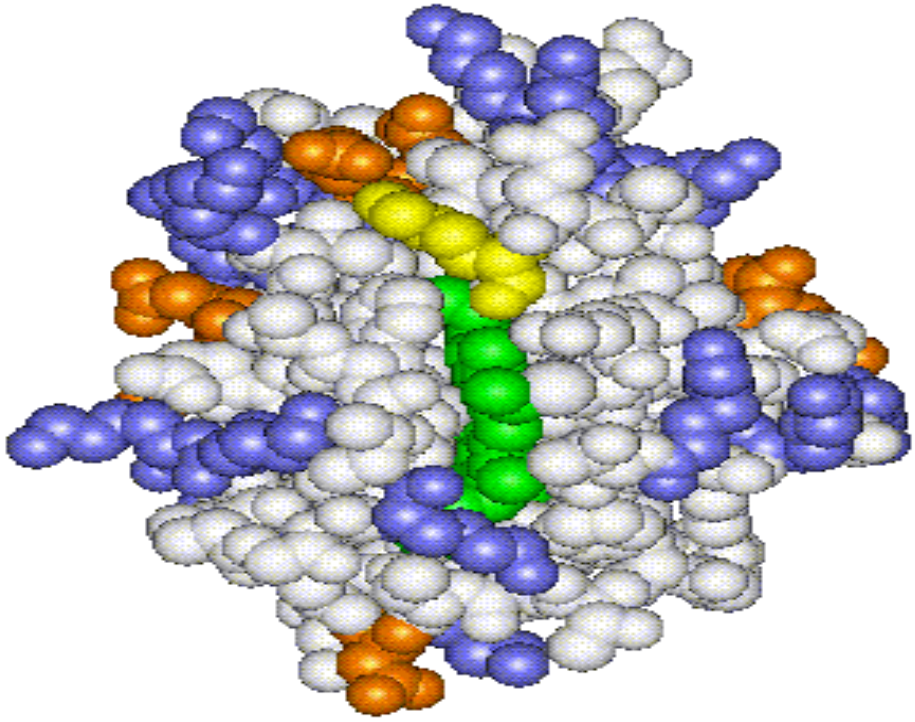

Figure 1.6. Space filled model of horse cytochrome *c* showing the positively charged lysine and arginine, shown in blue, near the to the heme, shown in green. Lysine 13 is shown in yellow and negatively charged glutamate and aspartate are shown in red. The structure was obtained from the Protein Data Bank under the protein code 1HRC[28].

1.4. REFERENCES

(1) Nuzzo, R. G.; Allara, D. L. *J. Am. Chem. Soc.* **1983**, *105*, 4481-4483.

(2) Tsai, M. Y.; Lin, J. C. *J. Biomed. Mater. Res.* **2001**, *55*, 554-565.

(3) Whitesides, G. M.; Laibinis, P. E. *Langmuir* **1990**, *6*, 87-96.

(4) Sondaghuethorst, J. A. M.; Fokkink, L. G. J. *Langmuir* **1992**, *8*, 2560-2566.

(5) Choi, J.; Morishita, H.; Kato, T. *Appl. Surf. Sci.* **2004**, *228*, 191-200.

(6) Prime, K. L.; Whitesides, G. M. *Science* **1991**, *252*, 1164-1167.

(7) Yan, L.; Marzolin, C.; Terfort, A.; Whitesides, G. M. *Langmuir* **1997**, *13*, 6704-6712.

(8) Whelan, C. M.; Kinsella, M.; Ho, H. M.; Maex, K. *J. Electrochem. Soc.* **2004**, *151*, B33-B38.

(9) Rickert, J.; Weiss, T.; Kraas, W.; Jung, G.; Gopel, W. *Biosens. Bioelectron.* **1996**, *11*, 591-598.

(10) Armstrong, F. A. *Struct. Bond.* **1990**, *72*, 137-230.

(11) Hawkridge, F. M.; Taniguchi, I. *Comments Inorganic Chem.* **1995**, *17*, 163-187.

(12) Fedurco, M. *Coord. Chem. Rev.* **2000**, *209*, 263-331.

(13) Folkers, J. P.; Laibinis, P. E.; Whitesides, G. M. *Langmuir* **1992**, *8*, 1330-1341.

(14) Song, S.; Clark, R. A.; Bowden, E. F.; Tarlov, M. J. *J. Phys. Chem.* **1993**, *97*, 6564-6572.

(15) Tarlov, M. J.; Bowden, E. F. *J. Am. Chem. Soc.* **1991**, *113*, 1847-1849.

(16) Eddowes, M. J.; Hill, H. A. O. *J. Chem. Soc.-Chem. Commun.* **1977**, 771-772.

(17) Yeh, P.; Kuwana, T. *Chem. Lett.* **1977**, 1145-1148.

(18) Chaubal, M. V.; Sen Gupta, A.; Lopina, S. T.; Bruley, D. F. *Crit. Rev. Ther. Drug Carr. Syst.* **2003**, *20*, 295-315.

(19) Bard, A. J.; Faulkner, L. R. *Electrochemical Methods: Fundamentals and Applications*; 2nd ed.; Wiley: New York, 2001.

(20) Schreiber, F. *Prog. Surf. Sci.* **2000**, *65*, 151-256.

(21) Ulman, A. *Chem. Rev.* **1996**, *96*, 1533-1554.

(22) Laibinis, P. E.; Whitesides, G. M. *J. Am. Chem. Soc.* **1992**, *114*, 1990-1995.

(23) Shimazu, K.; Yagi, I.; Sato, Y.; Uosaki, K. *J. Electroanal. Chem.* **1994**, *372*, 117-124.

(24) Brewer, S. H.; Brown, D. A.; Franzen, S. *Langmuir* **2002**, *18*, 6857-6865.

(25) Turyan, I.; Mandler, D. *Anal. Chem.* **1994**, *66*, 58-63.

(26) Schonenberger, C.; Jorritsma, J.; Sondaghuethorst, J. A. M.; Fokkink, L. G. J. *J. Phys. Chem.* **1995**, *99*, 3259-3271.

(27) Xu, W. S.; Zhou, H.; Regnier, F. E. *Anal. Chem.* **2003**, *75*, 1931-1940.

(28) http://www.rcsb.org/pdb/cgi/explore.cgi?pid=246041090522975&page=0&pdbId=1HRC

(29) Feng, Z. Q.; Imabayashi, S.; Kakiuchi, T.; Niki, K. *J. Electroanal. Chem.* **1995**, *394*, 149-154.

(30) Avila, A.; Gregory, B. W.; Niki, K.; Cotton, T. M. *J. Phys. Chem. B* **2000**, *104*, 2759-2766.

(31) Niki, K.; Hardy, W. R.; Hill, M. G.; Li, H.; Sprinkle, J. R.; Margoliash, E.; Fujita, K.; Tanimura, R.; Nakamura, N.; Ohno, H.; Richards, J. H.; Gray, H. B. *J. Phys. Chem. B* **2003**, *107*, 9947-9949.

CHAPTER 2

Synthesis and Characterization of 10-Mercaptodecanylphosphonic Acid

2.1. INTRODUCTION

The first major step in this longer term study has targeted the creation of phosphonate rather than phosphate SAMs due to the more straightforward synthesis. The 10-mercaptodecanylphosphonic acid ($C_{10}PA$) synthetic strategy followed a previously established procedure by Tsai et al[1] (scheme I).

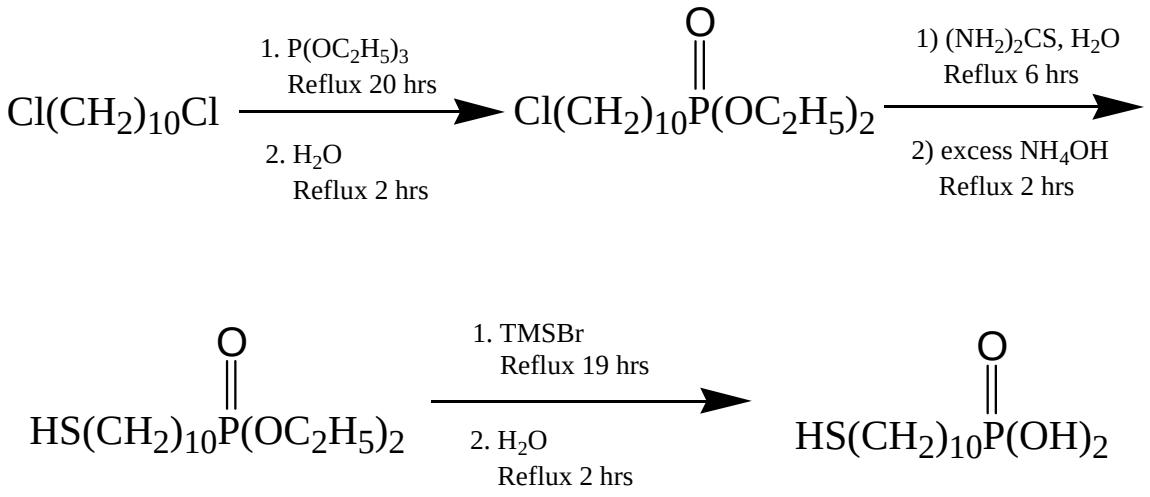

Scheme I. The steps for synthesizing 10-mercaptodecanylphosphonic acid.

2.2. MATERIALS AND SYNTHETIC PROCEDURES

2.2.1. Synthesis of Diethyl-10-Chlorodecanylphosphonate

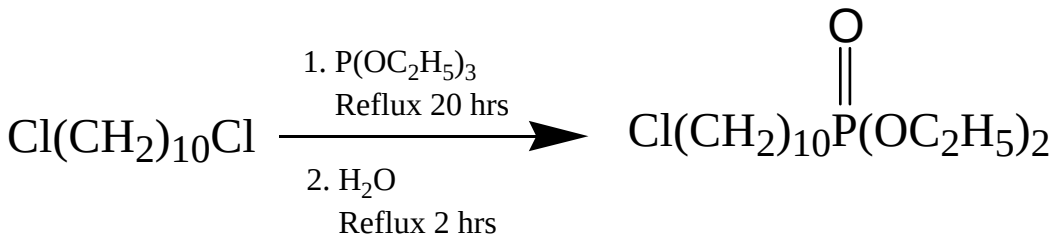

Reaction 2.1

The synthetic procedure for diethyl-10-chlorodecanylphosphonate is shown in Reaction 2.1. This simple Michaelis-Arbuzov reaction was kept under argon gas. Thirteen milliters (75.9 mmol) of triethyl phosphite was gradually added with a syringe into an argon-purged 100 mL 3-neck round bottom flask that already contained 12.73 g (60.3 mmol) of 1,10-dichlorodecane and a stir bar. The middle mouth of the 3-neck round bottom flask was attached to a reflux condenser and the two side mouths were covered with septa. The reaction mixture was refluxed for 20 hr in a 160 ^{o}C oil bath. The reaction mixture was then cooled to approximately 70^{o} C, 20 mL of water was added, and the contents were refluxed for another 2 hr. The reaction mixture was then extracted with approximately 150 mL of dichloromethane. The dichloromethane layer was washed with water, then brine (saturated NaCl), and dried over sodium sulfate. The filtered solution was concentrated in vacuo to a crude oil. The mass of the crude product obtained was 16.69 g (88% yield).

Purification

The crude product was purified on a chromatography column. A 1000 mL reservoir column of 300 mm length and 40 mm I.D. was packed with approximately 150 g of silica gel. The packing solvent was a 2:1 ratio of hexane to ethyl acetate. The expected R_f value is 0.53[1]. The target compound was monitored on a thin layer chromatography (TLC) plate. Since the diethyl 10-chlorodecanylphosphonate is not UV active, potassium permanganate solution was used to stain the TLC plate to visualize the spots.

For the first three column volumes, the elution solvent was a 2:1 mixture of hexane to ethyl acetate. Subsequent elution was carried out using a 1.5:1 ratio of hexane to ethyl acetate. The first two fractions collected contained 100 mL each, after which 50 mL fractions were collected. After combining the fractions containing the target compound as determined by TLC, the solvent was removed by rotary evaporation under vacuum to yield an oil product. The yield of the compound obtained was 6.34 g (34% yield).

2.2.2. Synthesis of Diethyl-10-Mercaptodecanylphosphonate

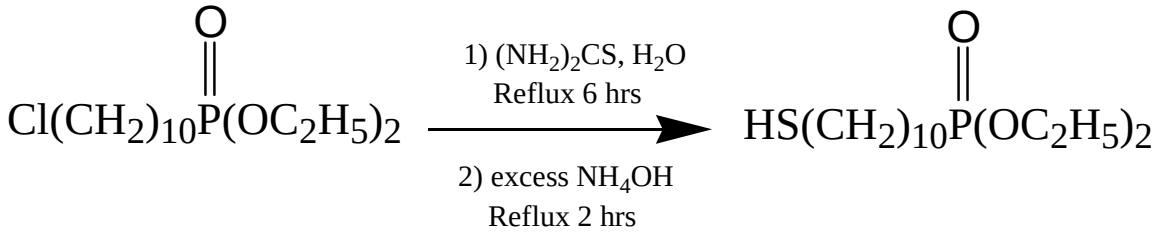

Reaction 2.2

The synthetic procedure for diethyl-10-mercaptodecanylphosphonate is shown in Reaction 2.2. A solution of 8.54 g (27.3 mmol) of diethyl-10-chlorodecanylphosphonate dissolved in 5 mL of ethanol was added to a 250 mL round bottom flask that contained 9.35 g (122.9 mmol) of thiourea. The reaction mixture was refluxed in an oil bath for 6 hr with stirring at 100 ^{o}C. The temperature was lowered to about 60^{o} C, approximately 15 mL of concentrated ammonium hydroxide was added with a syringe, and the mixture was heated for an additional 2 hr at 75 ^{o}C. After cooling to room temperature, the mixture was acidified with 10 wt % (3M) of aqueous HCl and refluxed for another 2 hr. The reaction mixture was then extracted with approximately 150 mL of ethyl acetate. The ethyl acetate layer was washed with 150 mL of water, brine (saturated NaCl), and then dried over sodium sulfate. The filtered solution was concentrated in vacuo to a crude oil with a mass of 6.04 g (95% yield).

Purification

The crude product was purified on a 1000 mL chromatography column packed with approximately 150 g of silica gel. The packing solvent used was a 7:1 ratio of hexane to ethyl acetate. The target compound was monitored on a thin layer chromatography plate and has an expected R_f value of 0.27[1]. Iodine vapor was used to visualize the eluted spots.

For the first three column volumes, the elution solvent was the 7:1 mixture of hexane to ethyl acetate. The polarity of the solvent was subsequently increased slowly to a 1:1 ratio of hexane: ethyl acetate. The first two fractions collected were 100 mL each, and after that, 50 mL fractions were collected. After combining the fractions containing the target compound as determined by TLC, the solvent was removed by rotary evaporation under vacuum to yield an oil product. The yield of the compound obtained was 3.10 g (50% yield).

2.2.3. Synthesis of 10-Mercaptodecanylphosphonic Acid

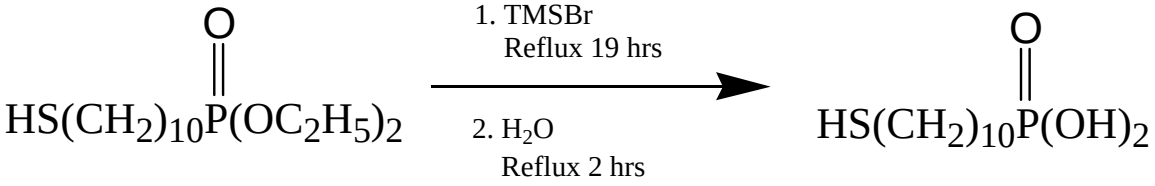

Reaction 2.3

The synthetic procedure for 10-mercaptodecanylphosphonic acid is shown in Reaction 2.3. To a 100 mL round bottom flask containing 3.08 grams (9.80 mmol) of diethyl-10-mercaptodecanyl phosphonate and a stir bar was added 3.83 mL (29 mmol) of bromotrimethylsilane using a syringe. Before adding any reagents to the round bottom flask, the flask was purged with argon gas for about 10 minutes. After stirring the reaction mixture at room temperature for 18 hours under argon gas, it was then refluxed for 1 hour. The reaction mixture was transferred to a 250 mL round bottom flask and excess reagent and solvent were removed in vacuo. The reaction mixture was then transferred into a 100 mL three-neck round bottom flask and 25 mL of deionized water was added. After hydrolyzing under argon gas for two hours, the reaction mixture was extracted with approximately 150 mL of methylene chloride. The methylene chloride layer was washed with water, brine (saturated NaCl), and then dried over sodium sulfate. The solvent was removed in vacuo and a flaky white crude product was obtained. The solid was redissolved with 5 mL of methylene chloride and recrystallized from hexane by storing in the refrigerator overnight. A pure, flaky, pearl white solid was obtained by suction filtration with a mass of 2.032 g (82% yield).

2.3. RESULTS

Analysis of Diethyl-10-Chlorodecanylphosphonate

^{1}H-NMR spectrum in $CDCl_3$ at 400 MHz: 1.35-1.210 ppm (overlapped, 18H), 1.58 (m, 2H), 1.65- 1.77 ppm (overlapped, 4H), 3.50 ppm (t, 2H), 4.11- 4.01 ppm (m, 4H).

Analysis of Diethyl-10-Mercaptodecanylphosphonate

^{1}H-NMR spectrum in $CDCl_3$ at 400 MHz: 1.26-1.70 ppm (overlapped, 25H), 2.46-2.53 ppm (q, 2H), 4.03-4.1 ppm (m, 4H).

Infrared (IR) spectrum features CH stretches at 2976.7 cm^{-1}, 2927.3 cm^{-1}, 2854.3 cm^{-1} in addition to the HS stretch at 2545.0 cm^{-1}. The IR spectrum was acquired primarily to confirm the formation of thiol in the reaction.

Elemental analysis yielded weight percents of [C] 54.16% and [H] 10.07%, which are consistent with the calculated composition of $C_{14}H_{31}O_3PS$: [C] 53.75%, [H] 10.25%.

Analysis of 10-Mercaptodecanylphosphonic Acid

^{1}H-NMR spectrum in $CDCl_3$ at 400 MHz: 1.27-1.62 ppm (overlapped, 19H), 2.49-2.55 ppm (q, 2H), 6.8 ppm (s, broad, 2H).

Elemental analysis yielded weight percents of [C] 47.23% and [H] 9.12%, which are consistent with the calculated composition for $C_{10}H_{23}O_3PS$: [C] 47.34% and [H] 9.14%.

FAB-MS m/z (nitrobenzyl alcohol matrix): High-resolution mass spectroscopy was carried out on the 10-mercaptodecanylphosphonic acid sample and the expected

molecular ion was observed at 255.1181 m/z (MH^+). The theoretical mass was 255.1184 m/z.

The melting point was determined to be 91.5 - 92^o C.

2.4. CONCLUSIONS

The synthesis and characterization of 10-mercaptodecanylphosphonic acid has been achieved. Results from proton NMR, infrared spectroscopy, mass spectroscopy and elemental analysis indicated that the compound was obtained in a highly pure form. Molecular weight was confirmed by high resolution mass spectroscopy. Data collected were consistent with the literature.[1]

2.5. REFERENCE

(1) Tsai, M. Y.; Lin, J. C. *J. Biomed. Mater. Res.* **2001**, *55*, 554-565.

CHAPTER 3

Surface Electrochemical Characterization of Cytochrome *c* Adsorbed on a Pure Phosphonic Acid Terminated SAM

3.1. INTRODUCTION

The goal of this research was to develop and study an electrochemical interfacial system that is closely related to biological interfaces. Bowden and coworkers[1-4] and other research groups[5,6] have previously studied cytochrome *c* (cyt *c*) adsorption and electroactivity using carboxylic acid (COOH) terminated SAMs. At physiological pH, some of the COOH terminal groups deprotonate forming a negatively charged surface, which makes it possible for electrostatic adsorption of positively charged redox species such as cyt *c* to occur. A pKa value of approximately 6 is usually observed for pure COOH SAM[3] on microscopically rough gold surfaces. The surface pKa can, however, be much higher on atomically flatter gold substrates, and this effect has been attributed to stronger hydrogen bonding between COOH groups[3]. Carboxylic acid terminated alkanelthiols adsorb on gold (specifically Au(111)) with a tilt angle of approximately 30^{o} and exhibit greater disorder compared to unsubstituted akanelthiols SAMs[7,8]. Researchers have proposed that hydrogen bonding between COOH termini occurs at an early stage of SAM assembly and leads to the observed disorder[7,8].

Figure 3.1 pictures 10-mercaptodecanylphosphonic acid (denoted as C_{10}PA), the molecule of interest in this thesis, while 11-mercapto-1-undecanoic acid (denoted as C_{10}COOH), the molecule that C_{10}PA will be compared with, is pictured in Figure 3.2. Both molecules feature the same C_{10} chain length.

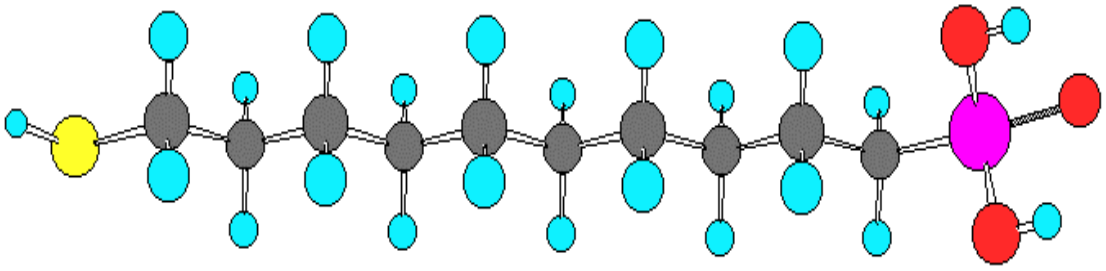

Figure 3.1. Structure of 10-mercaptodecanylphosphonic acid, $HS(CH_2)_{10}PO(OH)_2$.

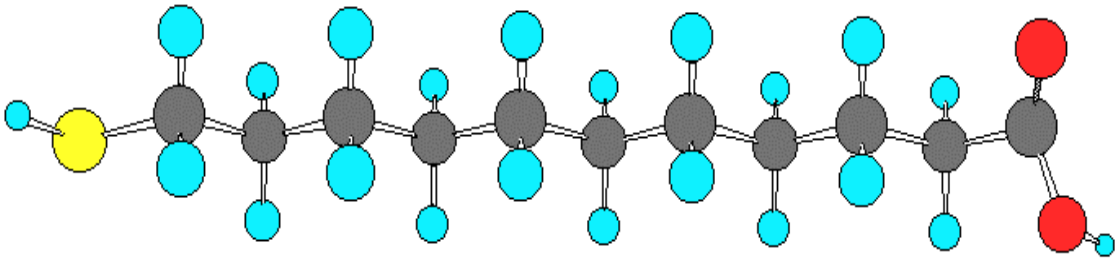

Figure 3.2. Structure of 11-mercapto-1-undecanoic acid, $HS(CH_2)_{10}COOH$.

It is anticipated that the thiol group of $C_{10}PA$ will attach to gold substrates leading to the formation of a self-assembled monolayer with the phosphonate group exposed to the solution. In neutral aqueous solutions some of the phosphonic acid groups are expected to ionize, which would make the modified surface negatively charged, as is the case for COOH SAMs. One can therefore expect that the positively charged region of a cationic protein like cyt *c* would be electrostatically attracted to a negatively charged phosphonic acid surface, much like the COOH SAM.

Cyclic voltammetry (CV) has been shown to be a useful technique for determining the electrochemical properties of biological redox proteins. This chapter will focus on the use of cyclic voltammetry to study the adsorption and redox properties of cyt *c* on phosphonic acid terminated SAMs on gold surfaces. The following properties are of interest: surface coverage, Γ (pmol cm^{-2}), standard electron transfer rate constant, k_{et}^{o} (s^{-1}), formal potential, $E^{o'}$(mV), double layer capacitance, C_{dl} (uF cm^{-2}), and an assessment of adsorbate dispersion as indicated by the peak width at half height, also known as the full width at half maximum, FWHM (mV).

3.2. EXPERIMENTAL PROCEDURES

3.2.1. Materials and Reagents

Horse heart cytochrome *c* (Type VI) was purchased from Sigma Chemical Company. The protein was purified on a cation exchange column[9] (Whatman C-52, Clifton, NJ) at 4°C. Water for all experiments was purified on a Milli-Q/Organex-Q system. 6-Mercapto-1-hexanol (C_6OH) and 11-Mercapto-1-undecanol ($C_{11}OH$) were purchased from Aldrich Chemical Company and used as received. 13-Mercapto-1-tridecanol ($C_{13}OH$) was synthesized previously by Russell Linderman's group at NCSU. 10-Mercaptodecanylphosphonic acid ($C_{10}PA$) was synthesized and purified according to previously established procedures[10]. The structure of $C_{10}PA$ was confirmed using proton NMR, infrared spectroscopy, elemental analysis, and high-resolution mass spectrometry (see Chapter 2).

3.2.2. Electrochemical Measurements

Electrochemical measurements were made with an EG&G (Princeton Applied Research) model 273A scanning potentiostat and a three-electrode system. A platinum wire served as the auxiliary electrode, Ag/AgCl (3M KCl) electrode (+0.207 V vs NHE) served as the reference electrode, and a monolayer modified gold electrode served as the working electrode. Cyclic voltammograms were acquired and used to determine double layer capacitance, surface coverage, formal potential and electron transfer rate constants. The standard electron transfer rate constant was calculated using software created by Jim Willit based on Laviron's simplest theory[11].

3.2.3. Electrode Preparation

The gold working electrodes consisted of 1000 to 3000 Å of evaporated gold bonded to 50 Å titanium on glass slides and was bought from Evaporated Metal Films in Ithaca, NY. The gold electrodes were subjected to a thorough cleaning process prior to SAM assembly on the electrodes. The first step of the cleaning process consisted of a 10-minute ultrasonication in 1% Liqui-Nox detergent followed by two 10-minute sonications in Milli-Q water. The gold electrode was then assembled into the electrochemical cell shown in Figure 3.3.

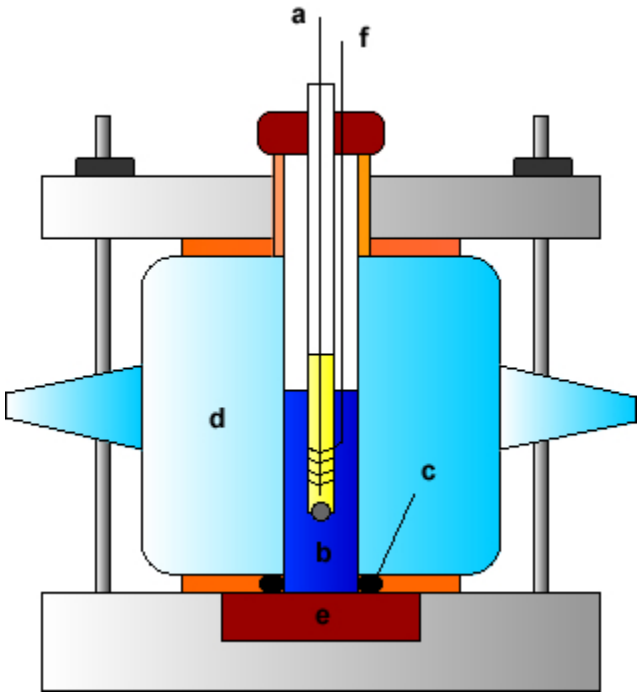

Figure 3.3. Diagram of the electrochemical cell. (a) Ag/AgCl reference electrode (glass barrel filled with 3M KCl); (b) buffered electrolyte solution; (c) viton O-ring; (d) glass cell body; (e) SAM modified gold electrode; (f) platinum wire auxiliary electrode.

The electrochemical cell was held together by a Lucite retainer. The surface area of the electrode (0.32 cm^2) corresponds to the area of the hole in the O-ring upon compression. For the second step of the cleaning process, the cell was filled with approximately 0.5 mL of 0.1 M H_2SO_4/ 0.01 M KCl solution. The reference and auxiliary electrodes were placed in closed proximity to the working electrode and the electrode was pretreated electrochemically by cycling the potential ten times between 0.0 mV to 1.5 mV vs Ag/AgCl[9,12]. The electrochemically pretreated gold electrode was rinsed 10 times with Milli-Q water, followed by rinsing 10 times with 95% ethanol.

3.2.4. Modification of Gold Electrode Surfaces

The cell was filled with a 5 mM pure C_{10}PA solution. The 5 mM homogenous solution of C_{10}PA was made by dissolving C_{10}PA solid in 95% ethanol solution. The SAM was then allowed to assemble at room temperature for 10 minutes to 3 days, depending on the experimental time desired.

3.2.5. Electrochemistry of Cytochrome c

After adsorption of thiols on gold substrate, the electrode was rinsed 10 times with 95% ethanol, follow by 10 times with Milli-Q water. The electrochemical cell was filled with 4.4 mM, pH 7 potassium phosphate buffer solution, which has an ionic strength of 10 mM, and a background scan was obtained. The buffer solution was then exchanged with a 12 μM cyt *c* solution prepared in the same buffer. Cytochrome *c* was

allowed to adsorb for 15 minutes, and the cell was then rinsed and filled with the phosphate buffer. Cyclic voltammograms were obtained at various scan rates.

3.3. RESULTS AND DISCUSSIONS

The background CV's obtained for a gold electrode before and after the formation of a pure C_{10}PA SAM are shown in Figure 3.4. The large decrease in charging current is typical for a well-formed SAM. The interfacial capacitance (double layer capacitance), C_{dl} (uF cm^{-2}), is obtained by dividing the total charging current, I_{tot} (amps), sum of the absolute values of the anodic and cathodic currents ($|I_{anodic}| + |I_{cathodic}|$), by the scan rate, ν (V/s), and electrode area, A (cm^2), at a specific potential (Equation 3.1). The C_{dl} value calculated for the pure C_{10}PA monolayer at a potential of 78 mV is 3.9 μF cm^{-2}.

$$C_{dl} = I_{tot}/ (2\upsilon A) \times 10^6 \qquad \textbf{Equation 3.1}$$

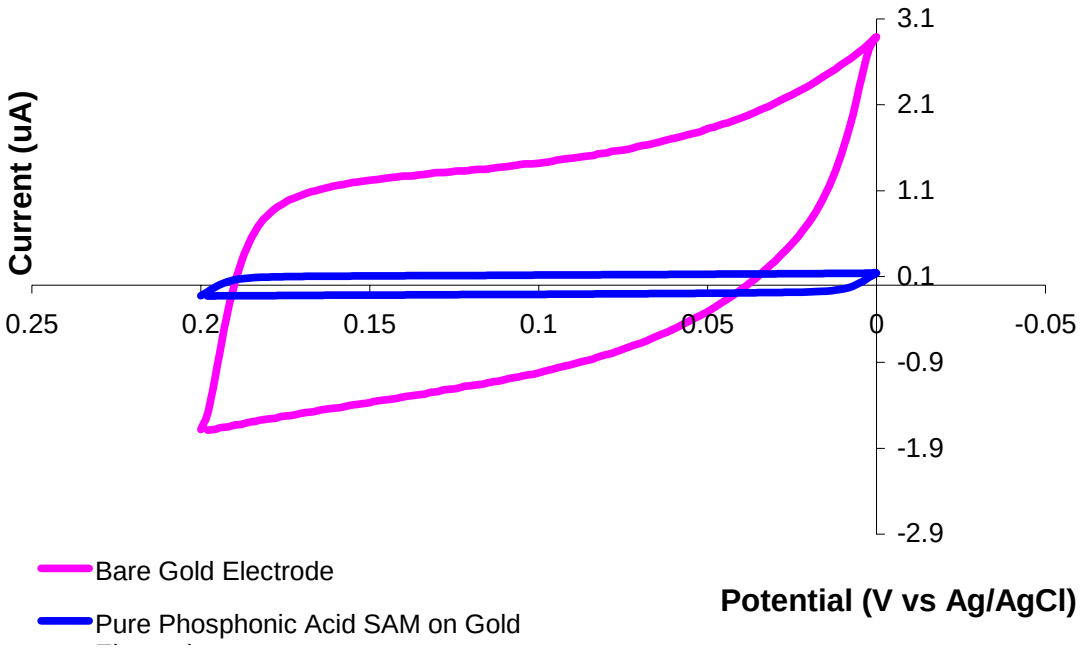

Figure 3.4. Cyclic voltammetry of background current of bare gold substrate and C_{10}PA SAM/gold substrate. The scan rate is 100 mV/s. The electrolyte solution is 4.4 mM potassium phosphate buffer, pH 7.0.

Following the acquisition of the background scan for the pure C_{10}PA SAM, the electrode was immersed in a cyt *c* adsorption solution for 15 minutes. The solution was then replaced with cytochrome-free, pH 7.0, 4.4 mM potassium phosphate electrolyte and CVs were obtained. The results are shown in Figure 3.5. Surprisingly, there are no observable voltammetric peaks between –0.2 V and 0.2 V vs Ag/AgCl that would indicate the presence of adsorbed cyt *c*.

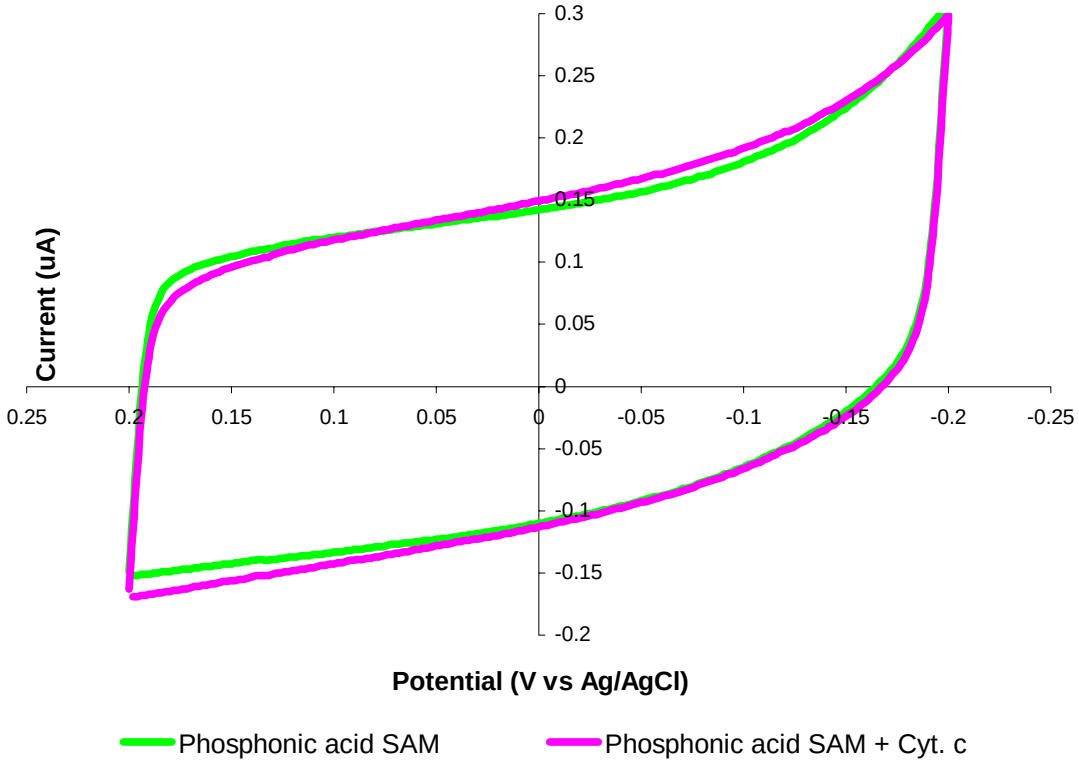

Figure 3.5. Cyclic voltammetry of a pure C_{10}PA SAM before and after exposure to a horse heart cytochrome *c* adsorption solution. The scan rate is 100 mV/s. The electrolyte solution is 4.4 mM potassium phosphate buffer, pH 7.0.

Figure 3.6 shows additional CVs at other scan rates for the same C_{10}PA monolayer after exposure to the cyt *c* adsorption solution. Again, no electroactive cyt *c* peaks were observed. Even at scan rates as low as 1 mV/s (not shown in figure), no faradaic response due to adsorbed cyt *c* was observed.

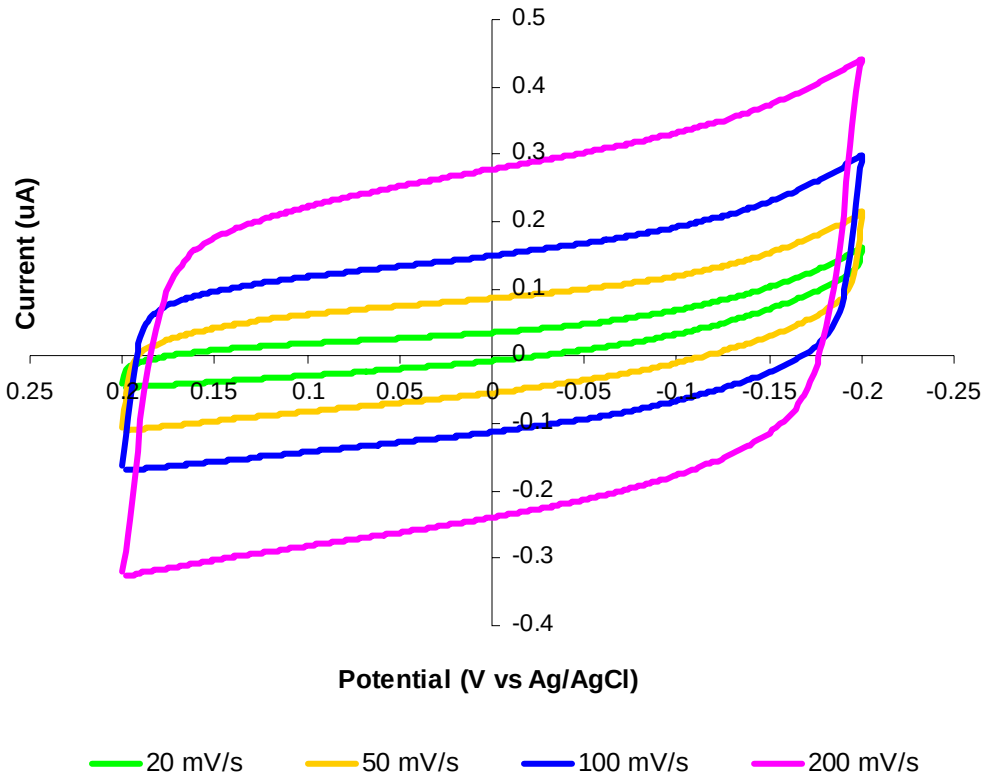

Figure 3.6. Cyclic voltammetry of a pure C_{10}PA SAM after exposure to a horse heart cytochrome *c* adsorption solution. The scan rate is 100 mV/s. The electrolyte solution is 4.4 mM potassium phosphate buffer, pH 7.0.

There are a few possible explanations for this observation. One possibility is that the surface of the monolayer is very cohesive due to strong hydrogen bonding and does not present a suitable binding environment for cyt *c*. This explanation would be similar to that previously proposed for the lack of cyt *c* response on pure COOH SAMs on atomically flat gold[3]. In that case, it was proposed that the pKa shifted to a significantly more basic value, resulting in minimal ionization of the COOH and therefore minimal adsorption of cyt *c*. X-ray photoelectron spectroscopy (XPS) results supported that view. In the present case, however, phosphonic acid groups are more acidic by approximately two pKa units and it would be surprising if the SAM surface were not extensively ionized. Thus adsorption of cyt *c* may be in fact occurring due to electrostatic interactions but not resulting in an electroactive state. Two possibilities to consider are denaturation of the adsorbed protein and/or poor electron communication between the cyt *c* heme and the gold electrode. Poor electronic communication might result from unfavorable orientation of cyt *c* on the SAM. Chen and co-workers[13] have reported that cyt *c* does adsorbed on sulfonate SAMs, but not in an electroactive state. However, their results are questionable because they determined that a bilayer of cyt *c* was present, a highly unusual result that may be related to impurities in their samples.

CONCLUSIONS

10-Mercaptodecanylphosphonic acid (C_{10}PA) forms stable and compact self-assembled monolayers on evaporated gold substrates. When C_{10}PA SAMs were exposed to cyt *c* solution, however, no electroactivity was observed even though favorable electrostatic interactions are expected. It is not clear whether cyt *c* is adsorbing in a nonelectroactive state or not adsorbing at all. Future experiments will address that issue. Because prior studies have shown that mixed SAMs with hydroxyl and carboxylic acid terminated thiols enhance the favorable binding of cyt *c*[2,4], similar studies were undertaken in this thesis using hydroxyl (OH)/phosphonic acid (PA) mixed SAMs. The results are presented in the next chapter.

3.4. REFERENCES

(1) Song, S.; Clark, R. A.; Bowden, E. F.; Tarlov, M. J. *Journal of Physical Chemistry* **1993**, *97*, 6564-6572.

(2) El Kasmi, A.; Wallace, J. M.; Bowden, E. F.; Binet, S. M.; Linderman, R. J. *Journal of the American Chemical Society* **1998**, *120*, 225-226.

(3) Leopold, M. C.; Black, J. A.; Bowden, E. F. *Langmuir* **2002**, *18*, 978-980.

(4) Leopold, M. C.; Bowden, E. F. *Langmuir* **2002**, *18*, 2239-2245.

(5) Arnold, S.; Feng, Z. Q.; Kakiuchi, T.; Knoll, W.; Niki, K. *Journal of Electroanalytical Chemistry* **1997**, *438*, 91-97.

(6) Avila, A.; Gregory, B. W.; Niki, K.; Cotton, T. M. *Journal of Physical Chemistry B* **2000**, *104*, 2759-2766.

(7) Dannenberger, O.; Weiss, K.; Himmel, H. J.; Jager, B.; Buck, M.; Woll, C. *Thin Solid Films* **1997**, *307*, 183-191.

(8) Himmel, H. J.; Weiss, K.; Jager, B.; Dannenberger, O.; Grunze, M.; Woll, C. *Langmuir* **1997**, *13*, 4943-4947.

(9) Leopold, M. C. In *Chemistry*; North Carolina State University: North Carolina, 2000.

(10) Tsai, M. Y.; Lin, J. C. *J. Biomed. Mater. Res.* **2001**, *55*, 554-565.

(11) Willit, J.; North Carolina State University: North Carolina, 1989.

(12) Nahir, T. M.; Bowden, E. F. *J. Electroanal. Chem.* **1996**, *410*, 9-13.

(13) Chen, X. X.; Ferrigno, R.; Yang, J.; Whitesides, G. A. *Langmuir* **2002**, *18*, 7009-7015.

CHAPTER 4

Surface Electrochemical Characterization of Cytochrome *c* Adsorbed on Hydroxyl/Phosphonic Acid Mixed SAMs

4.1. INTRODUCTION

SAMs composed of two different chain lengths and/or end groups, i.e., mixed SAMs, have been widely studied[1-3]. By using mixed SAMs, surface properties can be better controlled by employing two different terminal functionalities. Also, controlling the two chain lengths can affect the surface properties of mixed SAMs, with the shorter chain acting as a spacer while the longer chain protrudes with its end group exposed for possible binding interactions with redox proteins[4]. Cytochrome *c* (cyt *c*) adsorbed on gold electrodes modified with hydroxyl (OH)/carboxylic acid (COOH) mixed SAMs has been found to retain its electroactivity[5]. Faster rates of electron transfer were found when cyt *c* was adsorbed on OH/COOH mixed SAMs compared to adsorption on pure COOH SAMs[4-6]. Kasmi and Leopold [6, 7] from Bowden's group concluded that the electronic coupling between cyt *c* and SAMs can be enhanced through the use of SAMs composed of COOH terminated alkanethiols diluted with shorter OH terminated alkanethiols. These mixed monolayers have an advantage in that they allow the control of the degree and the charge on the monolayer surface.

Initial work in this thesis based on pure phosphonic acid ($C_{10}PA$) terminated monolayers showed no electroactivity for adsorbed cyt *c* (See Chapter 3). This lack of electroactivity could be due to: (1) the sp^3 hybridized, diprotic phosphonic acid terminal group hydrogen bonding extensively, perhaps limiting ionization needed for cyt *c* binding and/or rigidifying the interface; (2) cyt *c* binding so strongly to the SAM that it becomes denatured or oriented in an unfavorable position for electron transfer to take place. In this chapter, results of experiments utilizing mixed SAMs composed of hydroxyl alkanethiols (C_nOH; n = 6, 11, 13) and a phosphonic acid alkanethiol ($C_{10}PA$) are

presented. The hydroxyl alkanethiol serves as a hydrophilic diluent, spacing out the phosphonic acid groups and expected for feasible ionization with miminal hydrogen bonding. Thus can lead to electrostatic interaction between cyt *c* negatively charged mixed SAM interface at a favorable orientation for electron transfer to take place.

Hypothetical models of a pure C_{10}PA SAM and a C_{11}OH/C_{10}PA mixed SAM are presented in Figure 4.1 and 4.2 respectively.

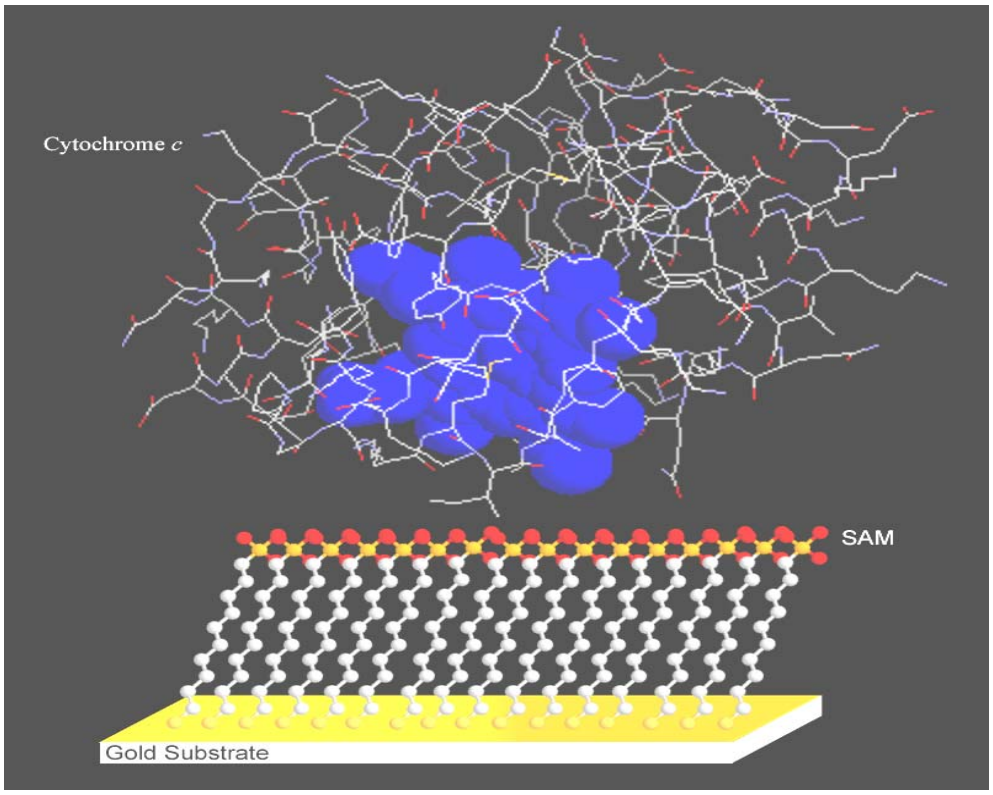

Figure 4.1. A proposed model of a pure C_{10}PA SAM on gold with a cytochrome *c* molecule positioned in a possible orientation assuming electrostatic binding. The possibility of significant interactions between phosphonic acid groups is evident in this schematic.

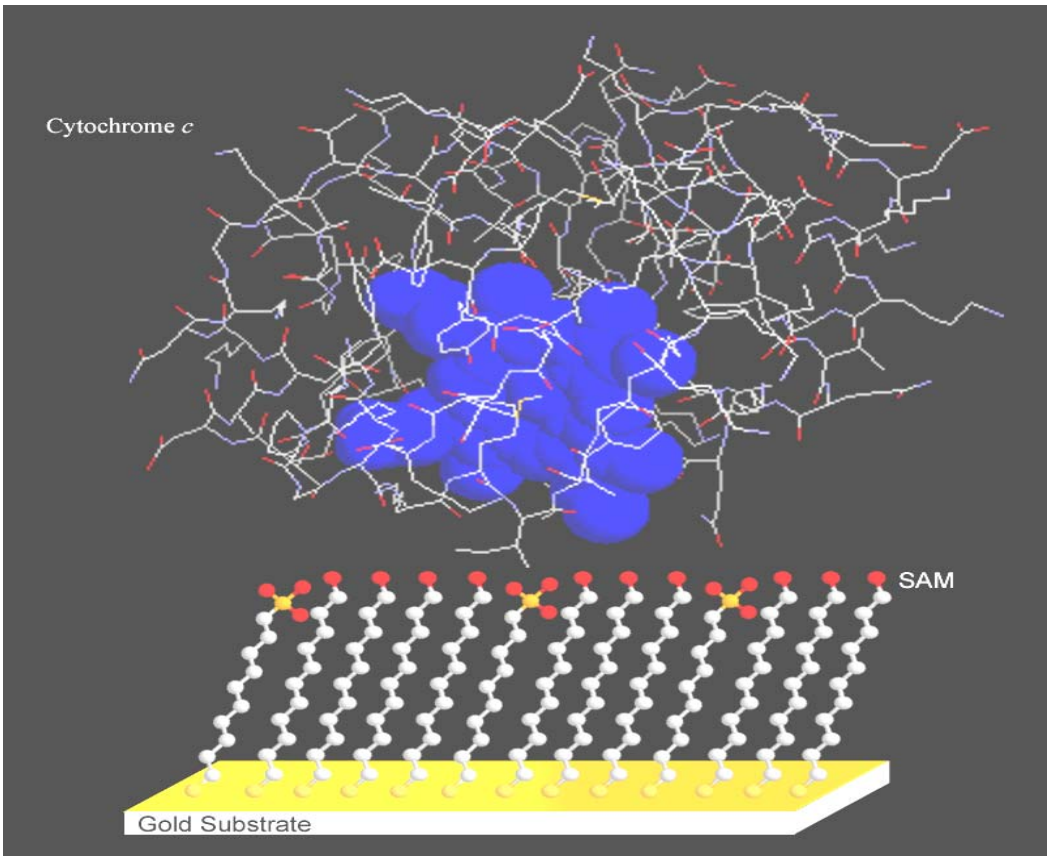

Figure 4.2. A proposed model of a $C_{11}OH/C_{10}PA$ mixed SAM on gold with a cytochrome *c* molecule positioned in a possible orientation assuming electrostatic binding. In this model, phosphonic groups can interact with hydroxyl groups but not with each other.

4.2. EXPERIMENTAL PROCEDURES

The experimental steps were preformed as described in Chapter 3. However, the gold electrode surfaces were modified with a 5 mM mixed $C_nOH/C_{10}PA$ (n = 6, 11, or 13) solution instead of the pure $C_{10}PA$ solution. The mixed thiol solutions were made by mixing the desired volume ratios of 5 mM $C_{10}PA$ and 5 mM C_nOH in 95% ethanol.

4.3. RESULTS AND DISCUSSION

The results and discussion section of this chapter will address voltammetric data obtained for adsorbed cytochrome *c* on a variety of hydroxyl/phosphonic acid mixed SAMs. The first three sections (4.3.1 - 4.3.3) describe results of a more qualitative nature in which the hydroxyl alkanethiol chain length, the mole ratio of hydroxyl thiol to phosphonic acid thiol, and the self-assembly time were systematically varied. From these experiments, an optimized system was determined, namely, a 10:1 ratio $C_{11}OH/C_{10}PA$ mixed SAM prepared with a 2-hour assembly time. In the final section (4.3.4), the results from a more detailed and quantitative characterization of the 10:1 $C_{11}OH/C_{10}PA$ mixed SAM will be presented. Determination of thermodynamic and electron transfer kinetic properties of adsorbed cyt *c* were obtained and compared to those obtained for a pure $C_{10}COOH$ SAM, which is of similar thickness.

4.3.1. Hydroxyl/Phosphonic Acid Mixed SAMs: Effect of Hydroxyl Thiol Chain Length

One has to consider the mole ratio of thiols, the terminal groups, and the chain lengths when making a mixed SAM. In this work, three different OH terminated alkanethiols ($HS(CH_2)_nOH$; n = 6, 11, 13) were mixed with 10-mercaptodecanylphosphonic acid ($C_{10}PA$). Figure 4.3 shows CVs of adsorbed cyt *c* on these three mixed SAMs; i.e., $C_6OH/C_{10}PA$, $C_{11}OH/C_{10}PA$, and $C_{13}OH/C_{10}PA$, in 4.4 mM potassium phosphate buffer, pH 7.0. The $C_{13}OH/C_{10}PA$ mixed SAM CV reveals very little adsorbed cyt *c* electroactivity. This result is undoubtedly related to the longer chain length of $C_{13}OH$, which would result in the $C_{10}PA$ phosphonic acid group being

buried within the monolayer and thus less accessible to cyt *c*. The lowered dielectric environment would also be expected to result in a more basic shift of the pKa, thus decreasing ionization further. On the other hand, $C_6OH/C_{10}PA$ and $C_{11}OH/C_{10}PA$ yield excellent cyt *c* electrochemistry, but the C_{dl} is much greater for the shorter hydroxyl chain. The C_{dl} for $C_6OH/C_{10}PA$ is almost twice as big as for $C_{11}OH/C_{10}PA$, which makes it more difficult to determine accurate baselines for background subtraction. Of the three different hydroxyl chain lengths that were mixed with $C_{10}PA$, the $C_{11}OH$ is clearly the best choice due to its smaller background and good cyt *c* coverage.

Other hydroxyl chain lengths (such as C_8OH, C_9OH, $C_{10}OH$, etc.) might give even better results with $C_{10}PA$. However, these are not readily available and need to be synthesized.

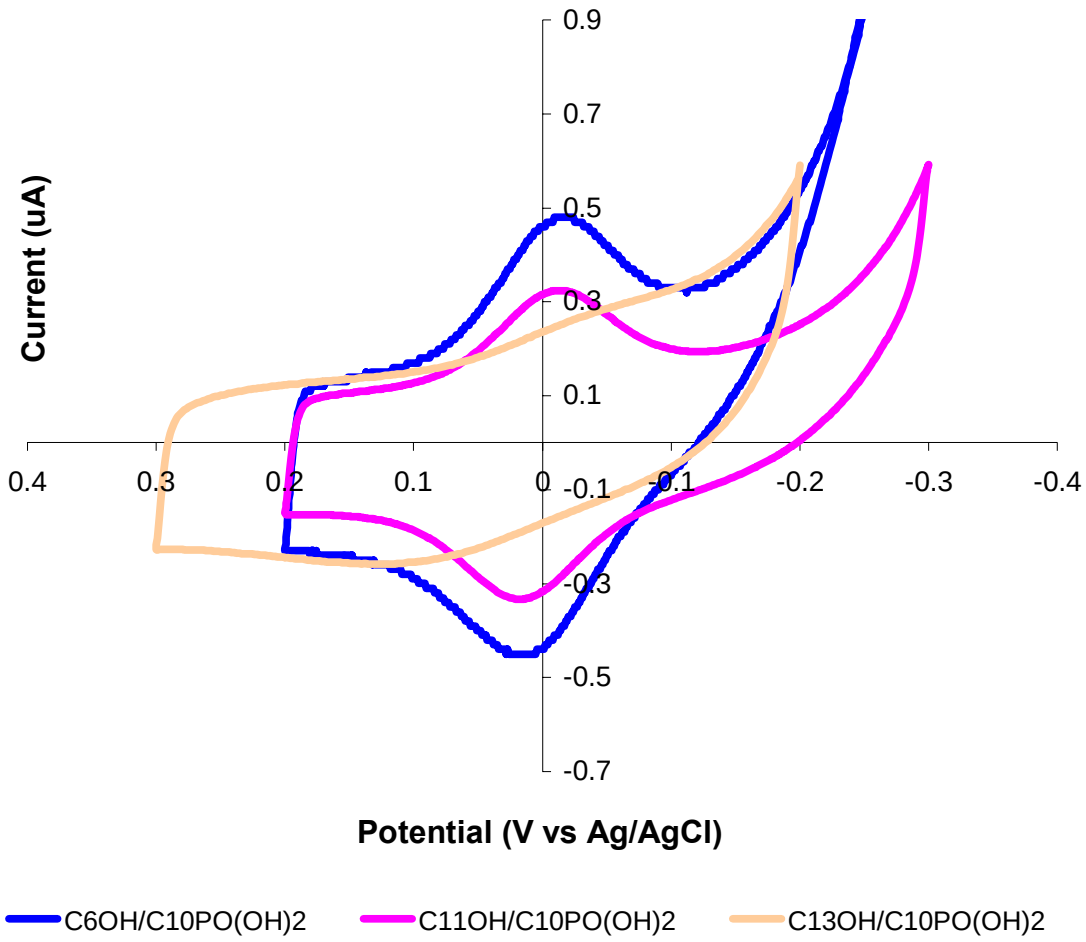

Figure 4.3. Cyclic voltammograms of cytochrome *c* adsorbed on $C_6OH/C_{10}PA$, $C_{11}OH/C_{10}PA$, and $C_{13}OH/C_{10}PA$ mixed SAMs at scan rate 100 mV/s.

4.3.2. $C_{11}OH/C_{10}PA$ Mixed SAM: Effect of Thiol Mole Ratio

Not only the terminal group and the chain length are important in self-assembly but also the thiol mole ratio in the self-assembly solution. Data presented here are for various mole ratios of $C_{11}OH$ and $C_{10}PA$. Mole ratio variation was also examined for C_6OH, $C_{13}OH$, and diethyl 10-mercaptodecanylphosphonate ($C_{10}PE$) thiols mixed with $C_{10}PA$, but the CV results were always inferior to the $C_{11}OH/C_{10}PA$ SAM and are not shown here. Figure 4.4 shows CVs of cyt *c* adsorbed on $C_{11}OH/C_{10}PA$ mixed SAMs prepared from solutions ranging from 2:1 to 50:1 ratios of $C_{11}OH$: $C_{10}PA$. The 50:1 $C_{11}OH/C_{10}PA$ ratio gave the worst results in terms of surface coverage. Other ratios evaluated, i.e., 2:1, 4:1, 10:1, resulted in similar electroactive coverage. However, the 2:1 ratio resulted in somewhat greater background current, which is undesirable from a data analysis perspective. Furthermore, the 2:1 ratio results in larger peak splitting and broader peaks than observed for the 4:1 and 10:1 ratios. Thus the ratios of 2:1 and 50:1 are clearly not optimal choices.

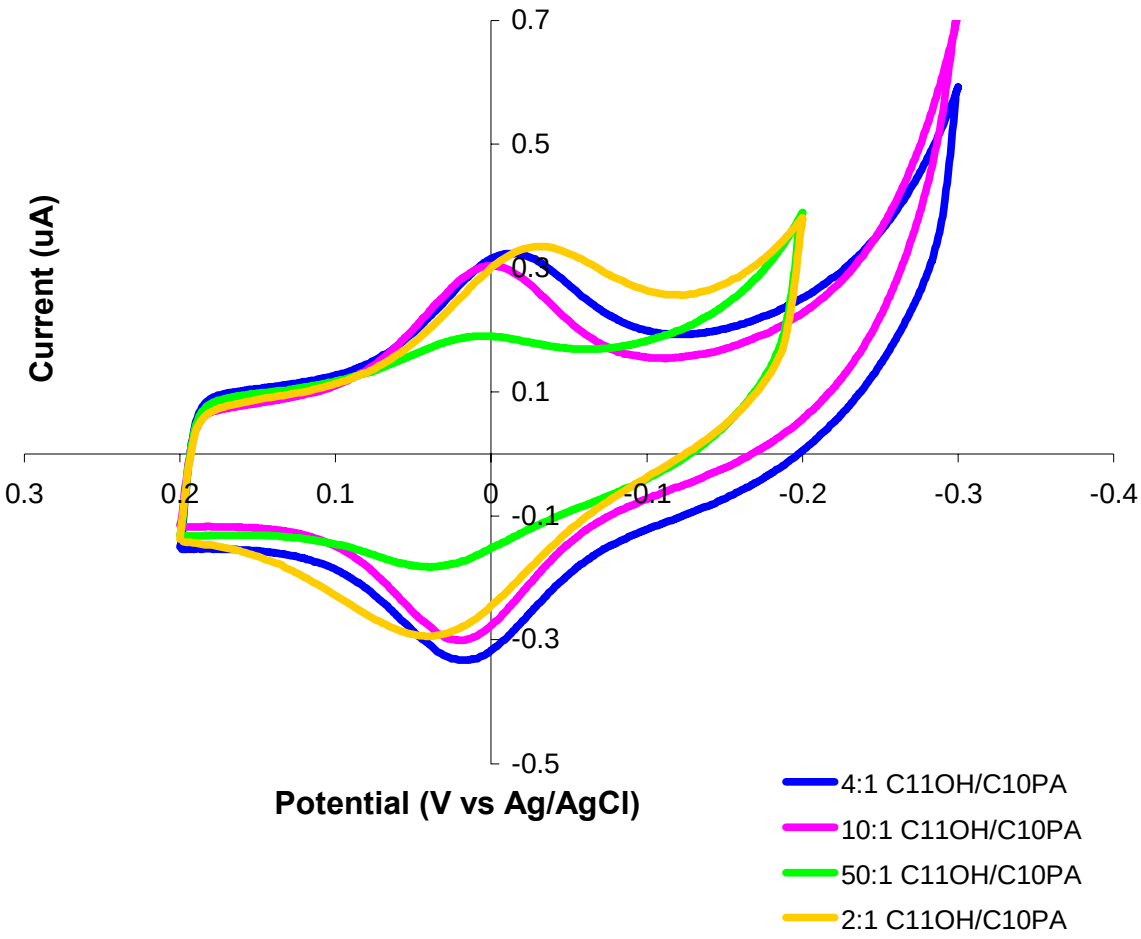

Figure 4.4. Comparison of cytochrome *c* responses on $C_{11}OH/C_{10}PA$ mixed SAMs assembled from various ratios of $C_{11}OH$ and $C_{10}PA$. All CVs were recorded at 100 mV/s. Overnight assembly was used.

Figure 4.5 presents a closer look at just the 4:1 and 10:1 $C_{11}OH/C_{10}PA$ results. Both CVs have similar adsorption peaks and background currents; however, the peak splitting is slightly smaller for the 10:1 ratio. The background current for the 10:1 ratio furthermore is slightly smaller than for the 4:1 ratio. The 10:1 ratio $C_{11}OH/C_{10}PA$ mixed

SAM is thus concluded to provide the optimal electrochemical response of those ratios evaluated and therefore was selected for further, more in-depth, characterization.

When there is too much $C_{11}OH$ relative to $C_{10}PA$, the SAM surface will have decreased negative charge density, which is the probable explanation for the poor results obtained with the 50:1 ratio. At the other extreme, when there is too little $C_{11}OH$, the SAM surface becomes too highly enriched in the $C_{10}PA$ component, and more closely approaches the structures of the pure phosphonic acid terminated SAM, which is a poor cyt *c* substrate as shown in the previous chapter.

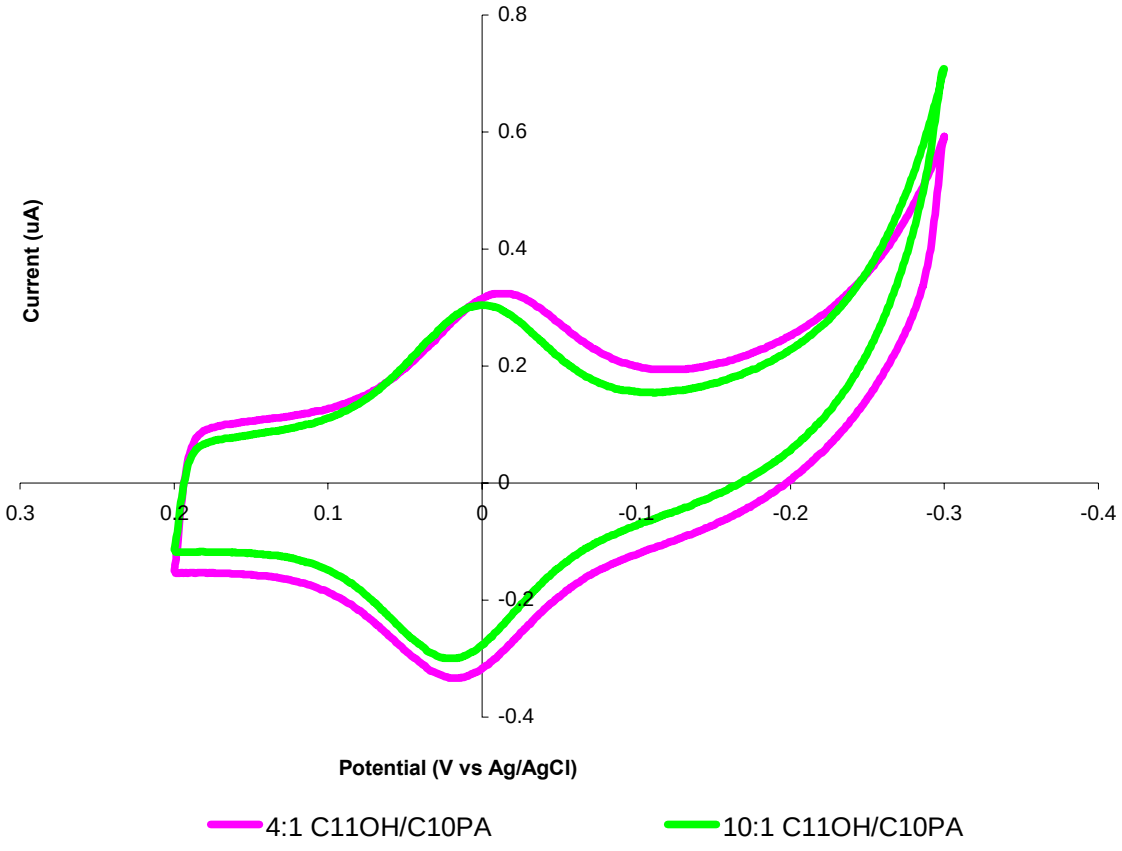

Figure 4.5. Cyclic voltammograms of 4:1 and 10:1 $C_{11}OH/C_{10}PA$ mixed SAMs. All CVs were recorded at 100 mV/s. Overnight assembly was used.

4.3.3. $C_{11}OH/C_{10}PA$ (10:1) Mixed SAM: Effect of Assembly Time

The time allowed for self-assembly can markedly affect the structure and properties of the resulting SAMs. In this experiment, 10:1 $C_{11}OH/C_{10}PA$ mixed SAMs were prepared at various assembly times, followed by a 15-minute adsorption of cyt *c*. Figure 4.6 shows CVs of adsorbed cyt *c* for self-assembly times of 10 minutes, 2 hours, 1 day, and 3 days. At 10 minutes, the background current is high and rises sharply for potentials below –0.05 V. This increased tailing is probably due to oxygen reduction. It is concluded that a 10-minute self-assembly does not result in a densely packed monolayer. However, CV results for 2 hours, 1 day, and 3 days are almost identical, which demonstrates that mixed SAMs of $C_{11}OH$ and $C_{10}PA$ form densely packed monolayers within a 2-hours of assembly time. Therefore, 2 hours was adopted as an adequate and efficient self-assembly time for further studies.

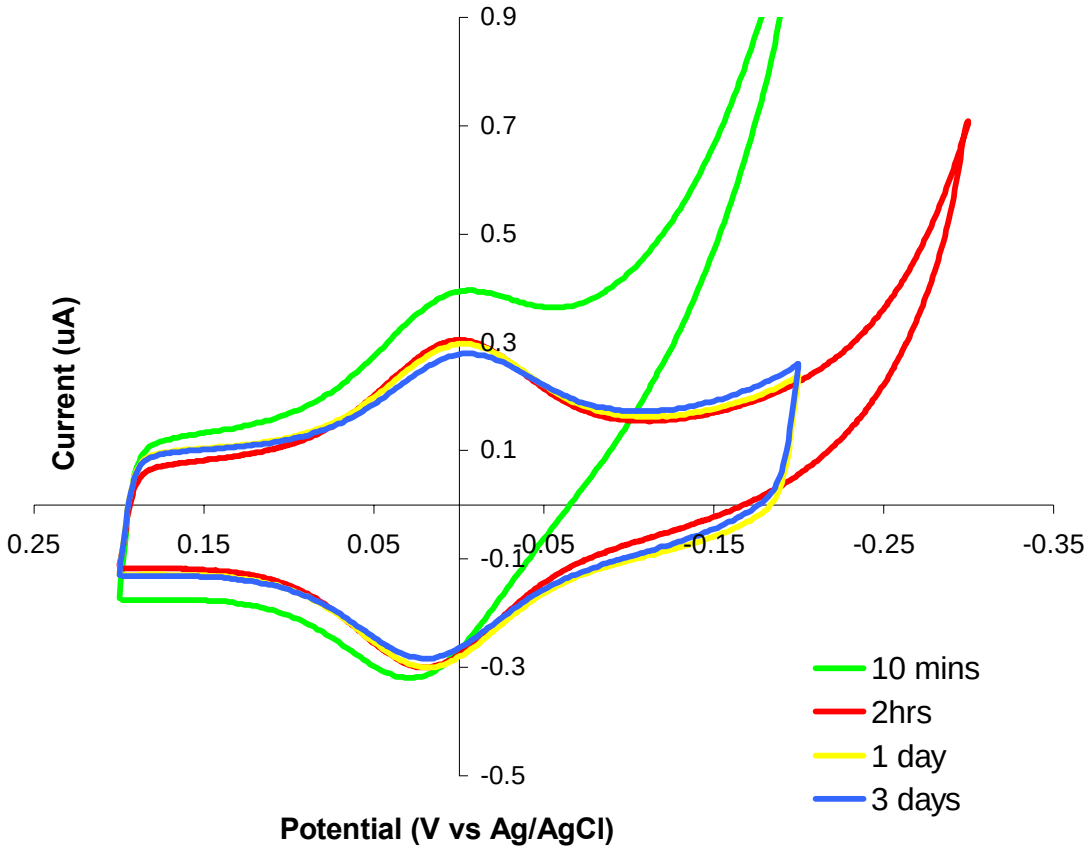

Figure 4.6. Cyclic voltammograms of cytochrome *c* responses for $C_{11}OH/C_{10}PA$ mixed SAMs showing the effect of self-assembly time.

4.3.4. Detailed Characterization of Adsorbed Cyt c on 10:1 $C_{11}OH/C_{10}PA$ Mixed SAM

In the previous sections, chain length, mole ratio, and self-assembly time were evaluated to determine an optimized set of conditions for a more quantitative characterization of adsorbed cyt *c*. From those studies, it was determined that a 10:1 $C_{11}OH/C_{10}PA$ mixed SAM prepared with a 2-hour self-assembly time was the best choice. All the results presented in this section were obtained using those conditions.

Figure 4.7 shows a typical 100 mV/s CV of adsorbed cyt *c* on a 10:1 $C_{11}OH/C_{10}PA$ mixed SAM in 4.4 mM phosphate buffer (pH = 7.0). The background obtained prior to cyt *c* adsorption is also shown. As expected, there were no voltammetric peaks observed within the potential window of interest prior to adsorption of cyt *c* on the modified gold electrode. After cyt c adsorption, a stable, well-behaved voltammetric response characteristic of an electroactive adsorbate appeared. This result indicated that cyt c adsorbs on these $C_{11}OH/C_{10}PA$ mixed SAMs with an orientation favorable for electron transfer.

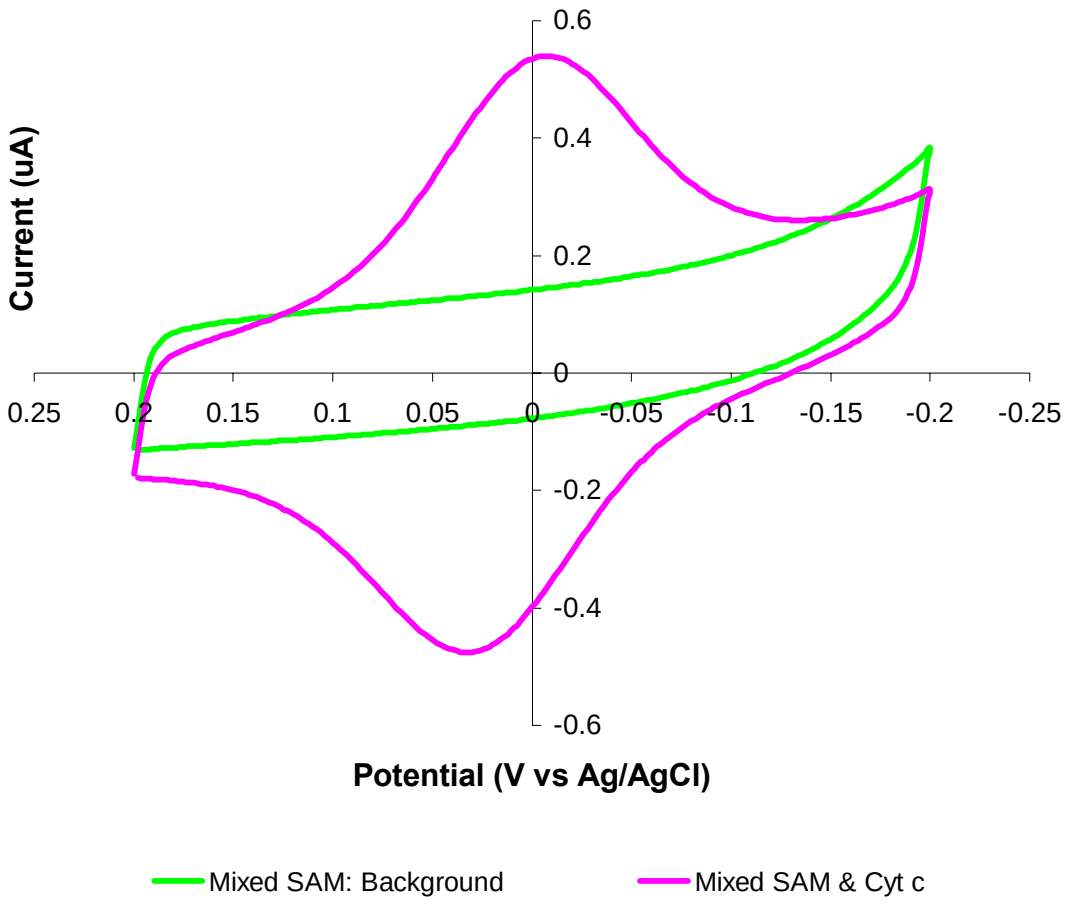

Figure 4.7. Cyclic voltammogram of horse heart cytochrome *c* adsorbed on 10:1 $C_{11}OH/C_{10}PA$ mixed SAM in 4.4 mM potassium phosphate buffer at 100 mV/s scan rate. Electrode area is 0.32 cm^2.

Figure 4.8 displays a series of cyclic voltammograms obtained at various scan rates for cyt *c* adsorbed on the $C_{11}OH/C_{10}PA$ mixed SAM. This behavior was reproducible and stable over a period of several hours. The CVs are comparable in quality to those observed on carboxylic acid SAMs[4, 8, 9] and can be used to determine redox properties for the adsorbed cyt *c*.

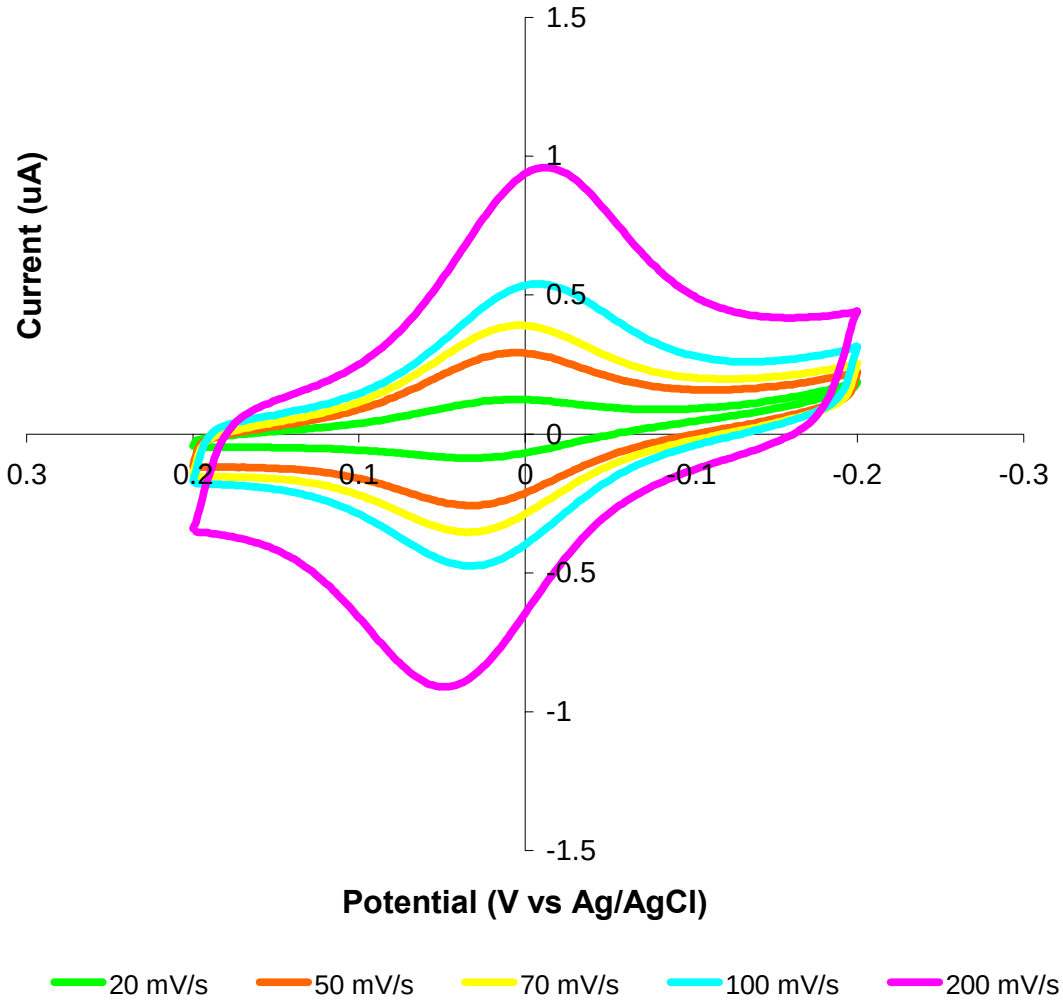

Figure 4.8. Cyclic voltammograms of adsorbed cytochrome *c* on the 10:1 $C_{11}OH/C_{10}PA$ mixed SAM at different scan rates.

Figure 4.9 shows the background-subtracted cathodic peak current, i_{pc}, as a function of scan rate. An approximately linear dependence of peak current on scan rate is consistent with the presence of cyt *c* immobilized on the surface.

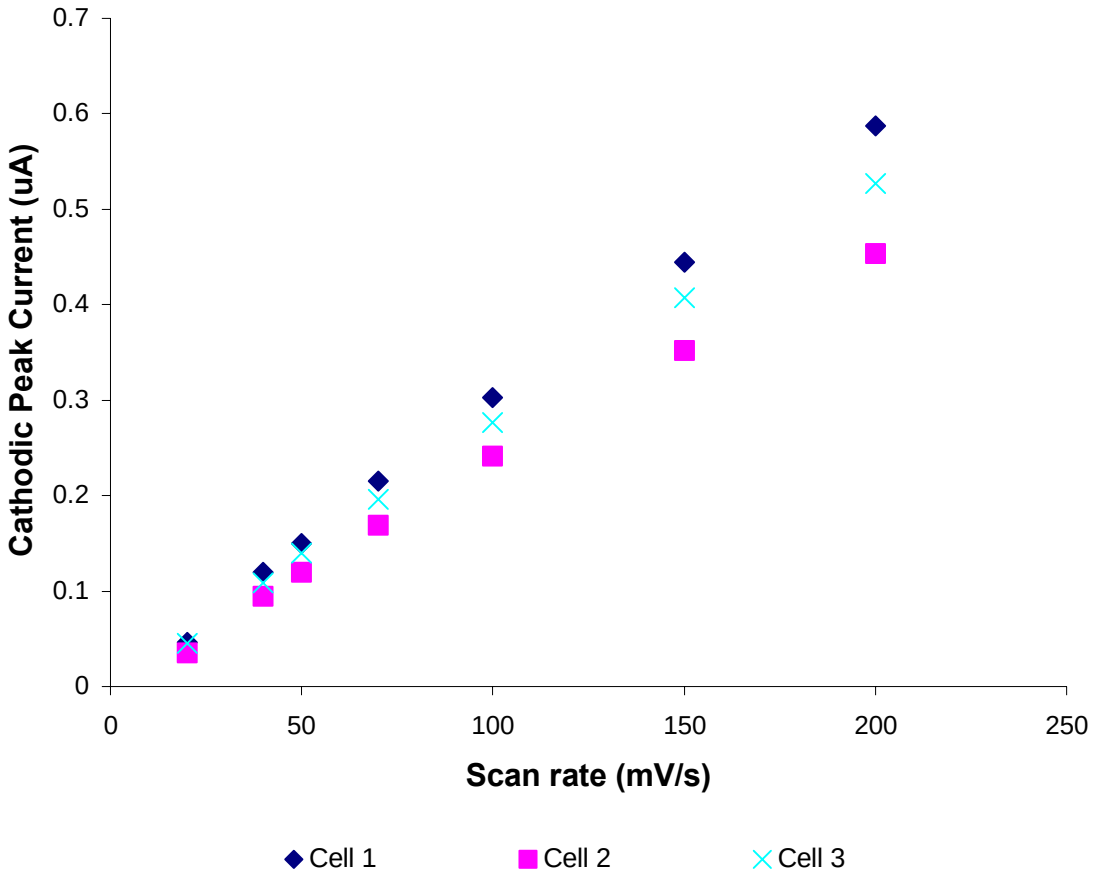

Figure 4.9. Plot of cathodic peak current (i_{pc}) versus scan rate.

CVs such as shown in Figures 4.7 and 4.8 can be analyzed for a number of important properties, including electroactive surface coverage (Γ), formal potential ($E^{o\prime}$), and the standard electron transfer rate constant (k_{et}^{o}) along with double layer capacitance (C_{dl}) and the peak full width at half-maximum (FWHM). The middle column in Table 4.1 presents those properties that were determined for 10:1 $C_{11}OH/C_{10}PA$ mixed SAMs that experiment through multiple repetitions, three data sets were obtained. Averages and standard deviations resulting from the three different electrodes are the numbers shown in Table 4.1. Also shown in the right hand column of the table, are results obtained in a similar manner for the well-studied $C_{10}COOH$ SAM. These are new data obtained for comparison with the mixed SAM results.

Before turning to the cyt *c* properties, we note that the dielectric properties of the $C_{11}OH/C_{10}PA$ and $C_{10}COOH$ SAMs are similar. Using equation 3.1 (See Chapter 3), the double layer capacitances were found to be 3.6 ± 0.3 uF cm^{-2} and 3.9 ± 0.3 uF cm^{-2} respectively at a potential of 78 mV. Considering the similar lengths of the thiols used to make these two SAMs, this result is not surprising. In both cases, well formed, densely packed SAMs, appear to be present.

Table 4.1. Electrochemical properties of adsorbed cytochrome *c*: 10:1 $C_{11}OH/C_{10}PA$ mixed SAM vs pure $C_{10}COOH$ SAM[a].

Property	**$C_{11}OH/C_{10}PA$ Mixed SAM**[b]	**$C_{10}COOH$ SAM**[b]
$E^{o'}$ (mV vs. Ag/AgCl)[c]	23 ± 1	21 ± 2
FWHM (mV)	103 ± 2	124 ± 2
Γ (pmol cm^{-2})[d]	9.7 ± 1.4	10.3 ± 1.1
Cdl (uF cm^{-2})	3.6 ± 0.3	3.9 ± 0.3
k_{et}^{o} (s^{-1})[e]	17.7 ± 3.6	12.7 ± 1.3

a) All measurements made in pH 7.0, 4.4 mM potassium phosphate buffer, following 15 minute cyt *c* adsorption period. Results shown with one standard deviation.
b) SAMs were assembled for 2 hours.
c) Formal potential is given versus Ag/AgCl (3 M KCl).
d) Surface coverage calculated from integrated charge under the cathodic peak.
e) Electron transfer rate constants were determined from cyclic voltammetric peak separations using Laviron's simplest model[10].

The electroactive surface coverage of cyt *c* was determined by integrating the charge under the cathodic peak after background subtraction. Using Faraday's Law[11]:

$$Q = nFA\Gamma \qquad \textbf{Equation 4.1}$$

Where Q is the total charge in coulombs, n is the number of electrons transferred, F is Faraday's constant, A is the area of the working electrode in cm^2, and Γ is the surface coverage in mol/cm^2. A value of 9.7 ± 1.4 $pmol/cm^2$ was obtained for the $C_{11}OH/C_{10}PA$ mixed SAM. This represents an estimated 65% of a monolayer, assuming 15 $pmol/cm^2$ is the value for full monolayer coverage[8]. A value of 10.3 ± 1.1 $pmol/cm^2$ was obtained for the pure $C_{10}COOH$ SAM, which is an acceptable result based on previous studies[8, 12]. Electroactive cyt *c* seems to adsorb to the same degree on both the $C_{11}OH/C_{10}PA$ mixed monolayer and the pure COOH monolayer.

The formal redox potential, $E^{o\prime}$(mV), of adsorbed cyt *c* was calculated as follows:

$$E^{o'} = (E_{pa} + E_{pc})/2 \qquad \textbf{Equation 4.2}$$

Where E_{pa} and E_{pc} are the anodic and cathodic peak potentials in mV, respectively. A value of 23 ± 1 mV vs Ag/AgCl (3 M KCl), or approximately 230 mV vs NHE, was obtained for $C_{11}OH/C_{10}PA$ mixed SAMs. This value agrees well with the formal potential of 21 ± 2 mV (~ 228 mV vs NHE) found for the $C_{11}COOH$ SAM. These two surface formal potentials are negatively shifted by –30 mV and –32 mV, respectively, from the solution value (~260 mV vs NHE) for horse cyt *c*. Shifts of this direction and

magnitude have been commonly observed for adsorbed cyt *c* on pure C_{11}COOH SAM[6, 13] indicating that the oxidized ferri (Fe^{3+}) form of cyt *c* binds more strongly than does the reduced ferro (Fe^{2+}) form.

The theoretical peak full width at half maximum height, FWHM (mV), for a reversible adsorbate is 90.6 mV at 25 ^{o}C for a simple one electron process[11]. The FWHM value calculated for adsorbed cyt *c* on the mixed SAM is 103 ± 2 mV, which is only some 10 mV larger than the theoretical value. On the other hand, the FWHM observed for the C_{10}COOH SAM is 124 ± 2 mV, which is significantly higher. Thermodynamic peak broadening for adsorbed proteins indicates the presence of a distribution of formal potential[13, 14]. From these results, the surface presented by the C_{11}OH/C_{10}PA mixed SAM can be concluded to be more homogeneous than the C_{10}COOH surface.

Laviron developed extensive theory for extracting electron transfer rate constants from CV data of redox adsorbates. In his simplest model, he assumes the equivalence of all adsorption sites, the absence of any adsorbate-adsorbate interactions, and an electron transfer rate that obeys Butler-Volmer kinetics[10]. Using this model, rate constants of 17.7 ± 3.6 s^{-1} and 12.7 ± 1.3 s^{-1} were obtained for the 10:1 C_{11}OH/C_{10}PA mixed SAM and the C_{10}COOH SAM, respectively, from evaluation of CV peak separation, ΔE_p (mV). Although the rate constant for the mixed SAM is slightly larger, there is not much contrast between the SAMs with regard to electron transfer kinetic behavior. Figure 4.10 is a plot of ΔE_p as a function of scan rate for three separate experiments. These ΔE_p values correspond to quasi-reversible electron transfer kinetics, which have splitting of < 200 mV.

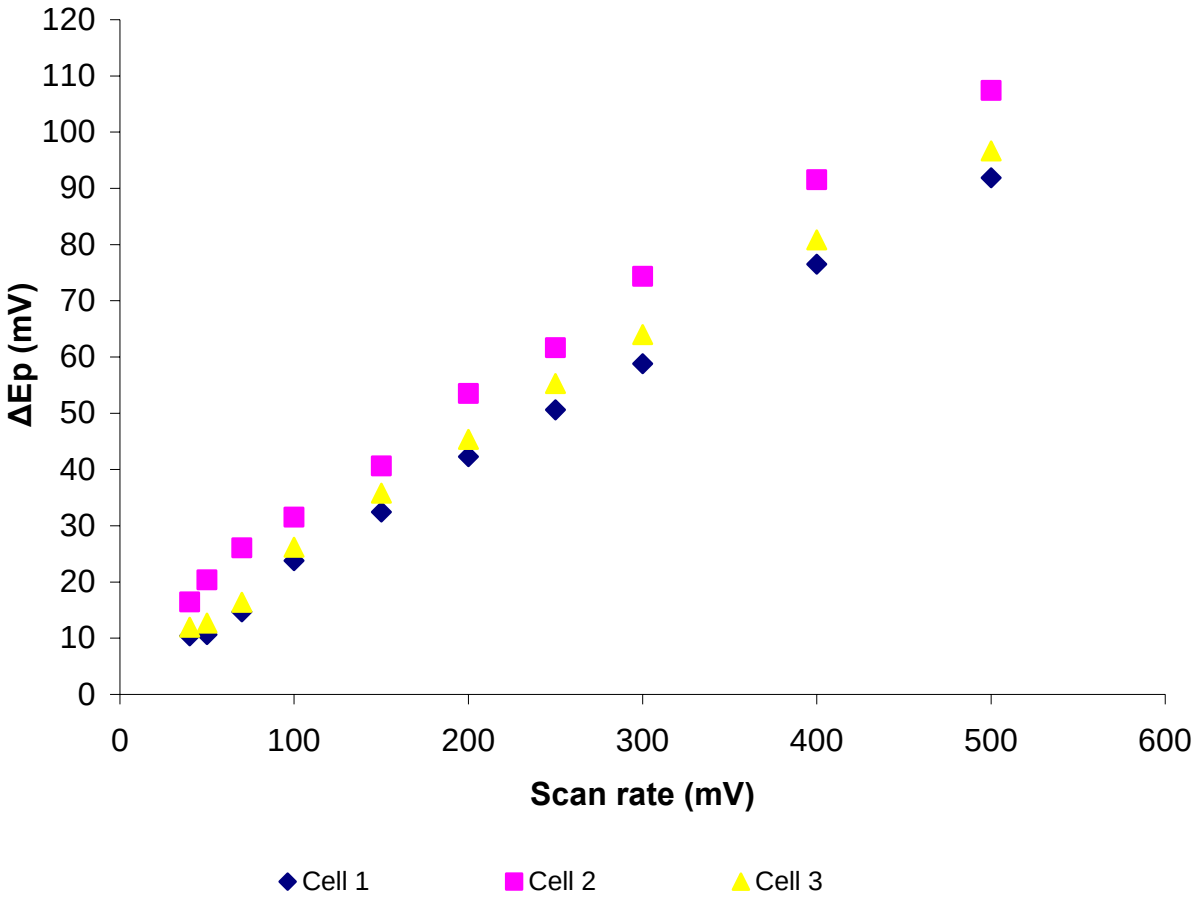

Figure 4.10. Peak separation (ΔE_p) vs scan rate for adsorbed cytochrome *c* on 10:1 $C_{11}OH/C_{10}PA$ mixed SAM for three different electrochemical cells.

Figure 4.11 is a plot of log k_{et}^{o} as a function of scan rate for three replicates. If Laviron's simplest model was completely valid, the rate constant should be independent of scan rate. In the figure, this is true but only at scan rate ≥ 400 mV/s, from which the rate constants reported above were obtained. At slower scan rate, Laviron's theory give rise to increasingly smaller values for the apparent rate constant. This type of behavior, which has been described previously, has been referred as unusual quasi-reversibility (UQR). The essential feature of UQR is a persistent, non-zero ΔE_p at the low scan rate limit that cannot be attributed to electron transfer kinetics. Since Laviron's model treats peak separation as arising entirely from electron transfer kinetics, it thus calculates erroneously small values of k_{et}^{o}. Laviron's simplest model is inadequate to describe the data obtained at scan rates ≤ 400 mV/s.

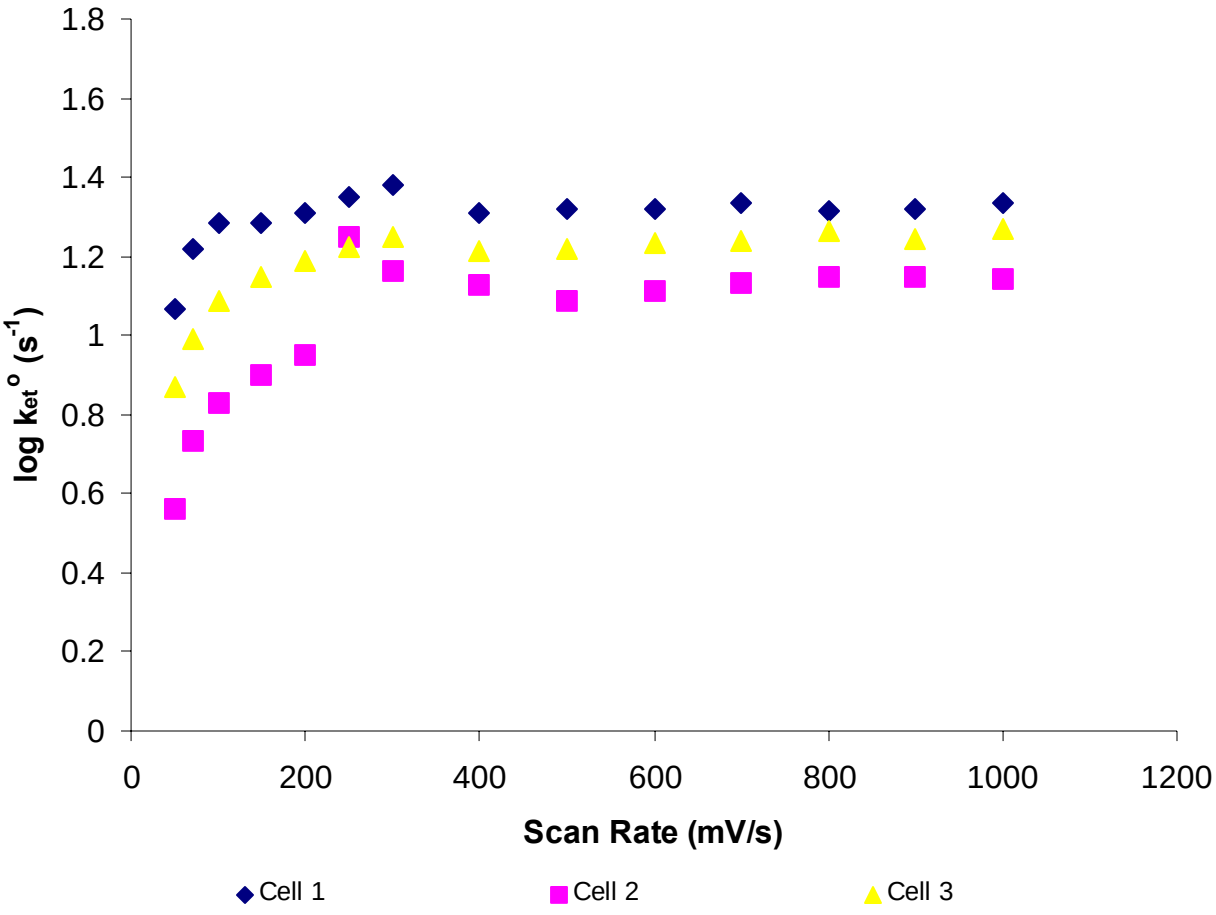

Figure 4.11. Standard electron transfer rate constant versus scan rate for adsorbed horse heart cytochrome *c* on 5 mM, 10:1 ratio $C_{11}OH/C_{10}PA$ mixed SAM.

To summarize, cytochrome *c* adsorbed on the $C_{11}OH/C_{10}PA$ mixed SAM exhibits redox properties that are comparable to those obtained for pure carboxylic acid terminated SAM of similar thickness, i.e., $C_{10}COOH$. The fact that cyt *c* adsorbs electroactively on $C_{11}OH/C_{10}PA$ mixed SAMs is a good initial step for investigating phosphate self-assembled monolayer.

4.4. CONCLUSIONS

The immobilization of horse heart cyt *c* on phosphonic acid self-assembled monolayers was investigated through electrochemical means. Attempts to adsorb cyt *c* electroactively on a pure C_{10} phosphonic acid SAM were completely unsuccessful. However, by combining phosphonic acid terminated alkanethiols with hydroxyl terminated alkanethiols, mixed SAMs were prepared onto which cyt *c* could be immobilized in a native electroactive state. A series of optimization experiments were conducted in which hydroxyl thiol chain length, mole ratio, and self-assembly time were varied. From those experiments, a 10:1 $C_{11}OH/C_{10}PA$ mixed SAM prepared with 2-hour self-assembly was selected for a more detailed characterization. On this mixed SAM, cyt *c* adsorbed in a stable, reproducible state. Overall, the redox properties of cyt *c* on the $C_{11}OH/C_{10}PA$ mixed SAM are quite similar to those obtained for a pure $C_{10}COOH$ SAM of similar thickness. It is concluded that $C_{11}OH/C_{10}PA$ mixed SAMs offer promising prospects for further investigations of electron-transfer behavior at the protein/electrode interface.

4.5. REFERENCES

(1) Bertilsson, L.; Liedberg, B. *Langmuir* **1993**, *9*, 141-149.

(2) Schonherr, H.; Ringsdorf, H.; Jaschke, M.; Butt, H. J.; Bamberg, E.; Allinson, H.; Evans, S. D. *Langmuir* **1996**, *12*, 3898-3904.

(3) Ulman, A. *Chemical Reviews* **1996**, *96*, 1533-1554.

(4) Arnold, S.; Feng, Z. Q.; Kakiuchi, T.; Knoll, W.; Niki, K. *Journal of Electroanalytical Chemistry* **1997**, *438*, 91-97.

(5) El Kasmi, A.; Leopold, M. C.; Galligan, R.; Robertson, R. T.; Saavedra, S. S.; El Kacemi, K.; Bowden, E. F. *Electrochemistry Communications* **2002**, *4*, 177-181.

(6) Leopold, M. C.; Bowden, E. F. *Langmuir* **2002**, *18*, 2239-2245.

(7) El Kasmi, A.; Wallace, J. M.; Bowden, E. F.; Binet, S. M.; Linderman, R. J. *Journal of the American Chemical Society* **1998**, *120*, 225-226.

(8) Song, S.; Clark, R. A.; Bowden, E. F.; Tarlov, M. J. *Journal of Physical Chemistry* **1993**, *97*, 6564-6572.

(9) Feng, Z. Q.; Imabayashi, S.; Kakiuchi, T.; Niki, K. *Journal of the Chemical Society-Faraday Transactions* **1997**, *93*, 1367-1370.

(10) Laviron, E. *Journal of Electroanalytical Chemistry* **1979**, *101*, 19-28.

(11) Bard, A. J.; Faulkner, L. R. *Electrochemical Methods: Fundamentals and Applications*, 2nd ed.; Wiley: New York, 2001.

(12) Feng, Z. Q.; Imabayashi, S.; Kakiuchi, T.; Niki, K. *Journal of Electroanalytical Chemistry* **1995**, *394*, 149-154.

(13) Clark, R. A.; Bowden, E. F. *Langmuir* **1997**, *13*, 559-565.

(14) Nahir, T. M.; Bowden, E. F. *Journal of Electroanalytical Chemistry* **1996**, *410*, 9-13.

CHAPTER 5

Future Directions

5.1. Future Directions

To further investigate the role of cyt *c* on 10-mercaptodecanyphosphonic acid SAMs, there is a need to better define the SAM structures and the interfacial interactions. Many techniques have been used to characterize SAM surfaces. Spectroscopy techniques such as surface infrared (IR) spectroscopy[1,2] , surface-enhanced Raman scattering (SERS) [3,4] surface plasmon resonance (SPR) spectroscopy[5,6], and X-ray photoelectron spectroscopy (XPS)[7] have been used to provides the orientation of the thiol chains, the thickness of the SAM, and surface coverage. Since no cyt *c* electroactivity was absent on pure C_{10}PA SAMs, it is important to gain molecular understanding of this SAM/protein interface. Scanning tunneling microscopy (STM)[8] and atomic force microscopy (AFM)[9] provide direct imaging of SAM structures, including defects or mixture of different structures during growth. Different CV results for adsorbed cyt *c* were observed for pure phosphonic acid SAM and hydroxyl/phosphonic acid mixed SAM suggesting that there could be extensive hydrogen bonding at the surface of the pure phophonic acid SAMs. In order to test this hypothesis, the use of other techniques is needed. In particular, the use of wetting contact angle[10] can be use to characterize the acid/base properties (pKa) of the surface. Ellipsometry[11] can be used to test for the presence of adsorbed cyt c.

As seen in the Results Section in Chapter 4, the C_{13}OH/C_{10}PA mixed SAM CV exhibits very little cyt *c* adsorption electroactivity. The longer C_{13}OH chain length may bury the C_{10}PA groups below the SAM surface, thus making it difficult for cyt *c* to bind. On the other hand, C_6OH/C_{10}PA mixed SAM CVs display comparable voltammetry to C_{11}OH/C_{10}PA, but the double-layer capacitance is much greater than the C_{11}OH/C_{10}PA SAM. Since it is known that chain length can dramatically affect SAM properties, it

would be desirable to test other chain length diluents such as C_8OH, C_9OH, and etc. The idea is to have OH thiols slightly shorter than $C_{10}PA$ to allow the phosphonic acid group to protrude out while minimizing the magnitude of the double-layer capacitance. These thiol molecules however need to be synthesized.

Results from preliminary tests of protein adsorption time (not shown in this thesis) suggested that longer cyt *c* adsorption leads to better surface coverage. More experiments need to be conducted to confirm this result.

As mentioned above, determining pKa value of the PA monolayers is an important objective. Contact angle measurements or infrared spectroscopy can be used for this task. Learning the pKa value is the key to understanding the charge state of the monolayer and its dependence on electrolyte composition, pH, and ionic strength.

5.2. REFERENCES

(1) Nuzzo, R. G.; Dubois, L. H.; Allara, D. L. *J. Am. Chem. Soc.* **1990**, *112*, 558-569.

(2) Parikh, A. N.; Allara, D. L. *J. Chem. Phys.* **1992**, *96*, 927-945.

(3) Thompson, W. R.; Pemberton, J. E. *Langmuir* **1995**, *11*, 1720-1725.

(4) Meuse, C. W.; Niaura, G.; Lewis, M. L.; Plant, A. L. *Langmuir* **1998**, *14*, 1604-1611.

(5) Aust, E. F.; Sawodny, M.; Ito, S.; Knoll, W. *Scanning* **1994**, *16*, 353-361.

(6) Peterlinz, K. A.; Georgiadis, R. *Langmuir* **1996**, *12*, 4731-4740.

(7) Martins, M. C. L.; Ratner, B. D.; Barbosa, M. A. *J. Biomed. Mater. Res. Part A* **2003**, *67A*, 158-171.

(8) Poirier, G. E. *Chem. Rev.* **1997**, *97*, 1117-1127.

(9) Tominaga, M.; Ohira, A.; Yamaguchi, Y.; Kunitake, M. *J. Electroanal. Chem.* **2004**, *566*, 323-329.

(10) Bain, C. D.; Whitesides, G. M. *Langmuir* **1989**, *5*, 1370-1378.

(11) Wasserman, S. R.; Whitesides, G. M.; Tidswell, I. M.; Ocko, B. M.; Pershan, P. S.; Axe, J. D. *J. Am. Chem. Soc.* **1989**, *111*, 5852-5861.